



<https://doi.org/10.11646/phytotaxa.419.1.3>

## Novel *Neidium* Pfitzer species from western Canada based upon morphology and plastid DNA sequences

PAUL B. HAMILTON<sup>1</sup>, AMANDA M. SAVOIE<sup>1</sup>, CYNTHIA M. SAYRE<sup>2</sup>, OLIVER SKIBBE<sup>3</sup>, JONAS ZIMMERMANN<sup>3</sup> & ROGER D. BULL<sup>1</sup>

<sup>1</sup> Canadian Museum of Nature, Station D, P.O. Box 3443, Ottawa Canada, K1P 6P4

<sup>2</sup> VanDusen Botanical Garden, 5251 Oak Street, Vancouver, British Columbia, Canada, V6M 4H1

<sup>3</sup> Botanischer Garten und Botanisches Museum Berlin, Freie Universität Berlin, Königin-Luise-Str. 6-8, 14195 Berlin, Germany

### Abstract

Five taxa in the genus *Neidium*, *N. iridis*, *N. beatyi* sp. nov., *N. vandusenense* sp. nov., *N. collare* sp. nov. and *N. lavoieanum* sp. nov. are documented from a pond and stream system in the VanDusen Botanical Garden, Vancouver, Canada. *Neidium beatyi* is a large linear species with multiple longitudinal canals and sagittate apices. The areolae are occluded by finger-like silica extensions on the external surface. This taxon is distinguished from *Neidium iridis* by the number of longitudinal canals (>5), shape of the valve apices, and smaller size. *Neidium vandusenense* is broadly linear with distinct rostrate apices. Two-three longitudinal canals are present along each margin. Plastid *rbcL* sequence data associates this taxon with *N. amphigomphus*. *Neidium collare* is an elliptic lanceolate taxon with one longitudinal canal. This taxon is genetically related to *N. biscalatum* sensu lato, but with a different shape form. *Neidium lavoieanum* has a valve shape form similar to *Neidium potapovae*, but is larger and genetically similar to *N. productum* sensu lato. The five *Neidium* taxa were observed in a small stream next to Lake Victoria (pond) in the VanDusen Botanical Garden Vancouver, Canada. The water was mildly alkaline with a pH of 7.86, a conductance of 163  $\mu\text{S}/\text{cm}$ , higher nutrient loads and low metal content.

### Introduction

The diatom genus *Neidium* Pfitzer (1871: 39) contains over 300 taxa (Guiry & Guiry 2019, VanLandingham 1978) with a diversified range in valve structure and a supported genetic phylogeny for the prominent taxa (e.g. Hamilton & Jahn 2005, Lefebvre & Hamilton 2015, Lefebvre *et al.*, 2016). The genus is morphologically based on cellular structure, and the four lobed cytological separated formation of the chloroplasts (Cox 1997). Cleve (1894) studied the valve morphology and made interesting observations on the proximal and distal raphe fissures, combined with unique longitudinal lines (now recognised as longitudinal canals) and oblique orientated punctated striae. Cleve also noted morphological similarities to *Scoliopleura schneideri* (Grun 1878: 113) Cleve (1894: 105) and *Caloneis* spp. At that time there was also a good understanding of auxospore and perizonium formation for the genus (Griffith 1855) with more recent detailed studies of auxospore formation (Mann 1984).

The identification of species in this genus has historically been problematic, with taxon identifications using a limited recognition of morphological structures resulting in type II errors (different taxa identified as the same). Indeed Cleve (1894) commented “The numerous forms included in *Neidium* are so intimately connected, that all the species are more or less artificial and founded on variable characteristics, such as the form and outline of the valve.” Reimer (1959) examined and identified many type taxa from historical collections acquiring excellent notes and commented on the morphology and problems associated with past taxa identifications. Some taxa are genetically and morphologically distinct (e.g. *N. hitchcockii* (Ehrenb. 1841: 418) Cleve (1894: 69)) (Hamilton & Poulin 1995, Lefebvre & Hamilton 2015) while other species have more limited character differentiation (e.g. Liu *et al.* 2000). At present the prominent identifying morphological character for the genus is scattered renilimbria (Figs 16 & 42 this study, black arrows), which are internally positioned spathulate hooks associated with areolae on the valve face and on the longitudinal canal (e.g. Hamilton & Jahn 2005, Hamilton *et al.* 2019, Liu *et al.* 2010). Genetically, the genus *Neidium* forms a defined clade separated from *Neidiomorpha* Cantonati *et al.* (2010: 196), *Luticola* D.G.Mann (Round *et al.* 1990: 670), *Biremis* D.G.Mann (Round *et al.* 1990: 664) and *Scoliopleura* Grun. (1860: 554) (Navkov *et al.* 2018) within the Neidiaceae.

In a routine sampling trip to western Canada, samples were collected containing five *Neidium* taxa with distinct valve morphology and genetics. *Neidium iridis* sensu stricto was identified along with four new taxa. This study documents and defines the ecology of the new species of *Neidium* with morphological and genetic study.

## Methods

Six samples for this study were collected from a narrow stream (49° 14' 22.75" N, 123° 07' 50.02" W) at the end of Livingstone Lake (pond) in the VanDusen Botanical Garden, Vancouver, Canada from 2016–2018. Samples were kept alive for transport back to the lab. In the lab, samples were split, with a subsample kept alive for DNA analysis and a second subsample subjected to processing for slide and material preservation. For long-term conservation, freeze-dried subsamples for morphological studies were deposited in the Canadian Museum of Nature Phycology Collection (CANA, 126257, 126425, 126426, 128318, 128327). A sample for water analysis was collected on January 24, 2019 from the sample site and analysed at the ALS Environmental Lab Vancouver B.C. for the City of Vancouver using QC lots 1031235, 1031567, 1031949, 1033243 and blanks. For specific methods in the analysis and lab Certificate of Analysis, see Supplement C.

**Morphological studies:**—Samples for morphological analysis were digested with hot H<sub>2</sub>SO<sub>4</sub>:HNO<sub>3</sub>. The samples were then treated through a series of dilutions (at least 5×) to remove oxidative by-products and residual acid. Subsamples from the treated slurries were dried onto microscope coverglass and mounted onto microscope slides using Naphrax®. Microscopic studies were conducted using a Leica DMR microscope equipped with a Pixelink digital camera or a Nikon Microphot-FX microscope with the same camera system. Specimens were observed at magnifications ranging from 640–1000× using NPlan or Plan Apo objectives (NA 1.25–1.35) with bright field (BF) and differential interference contrast (DIC) optics. Scanning electron microscopy preparations were made by drying a subsample of cleaned material onto aluminum foil and mounted onto aluminum stubs using double sided carbon tape. In some cases, individual valves were isolated and mounted on aluminum foil then using double sided carbon tape mounted on stubs. The mounted stubs were coated with ~500 Å of Au or Au-Pd and examined with an Apreo FEI field emission microscope (FEI, Hillsboro, USA) with accelerating voltages between 2–5 kV and working distances 3–10 mm. Both secondary electron and backscatter imaging was used. Morphological metrics include valve length, width, stria density, areola density, and number of canals. Fine structural details like termination of raphe ends, areolae structural formation, orientation of renilimbria and formation of helictoglossae were recorded. All terminology follows Stosch (1975), Krammer & Lange-Bertalot (1986) and Siver *et al.* (2003). Type specimens of each species were selected to best represent the general morphology of the population.

**Genetic studies:**—Single cell diatom isolations were used to conduct nested PCR and sequencing procedures following Hamilton *et al.* (2015). Sequences for outgroup taxa were determined from cultures following different protocols (Theriot *et al.* 2010). For genetic analyses cultures of two *Neidioromorpha* taxa (*Neidioromorpha binodis* (Ehrenb. 1840: 212) Cantonati *et al.* (2010: 200), *Neidioromorpha binodiformis* (Krammer in Krammer & Lange-Bertalot 1985: 102) Cantonati *et al.* (2010: 200)) were used as the sister outgroup (Table 2). Cultured material was transferred to 1.5mL tubes. The DNA was isolated using the NucleoSpin® Plant II Mini Kit (Macherey and Nagel, Düren, Germany) or Qiagen® Dneasy Plant Mini Kit (Qiagen, Valencia, CA) following the respective product instructions. The DNA fragment size and concentrations were measured via gel electrophoresis (1.5% agarose gel) and Nanodrop® (PeqLab Biotechnology, Erlangen, Germany), respectively. The DNA samples were stored at –20°C for future use and finally deposited in the Berlin collection of the DNA bank network (Droege *et al.* 2014). The polymerase chain reaction (PCR) for *rbcL* was conducted following Abarca *et al.* (2014). PCR products were visualized in a 1.5% agarose gel and cleaned with MSB SpinPCRapace® (Invitex LLC, Berlin, Germany) following standard procedures. DNA concentrations were measured using Nanodrop® (PeqLab Biotechnology) and samples were normalized to a total DNA content >100 ng µL<sup>-1</sup> for sequencing. Sanger sequencing was conducted by Star® (GENTERprise, Mainz, Germany), *rbcL* gene according to Abarca *et al.* (2014). Same primers were used for amplification and sequencing. The editing, as well as the quality control of the pherograms for the new sequences, were done in Phyde® (Müller *et al.* 2010). Additional outgroups, were retrieved from Genbank including *Scoliopleura peisonis* Grun. (1860: 554), and *Luticola ventricosa* (Kützing 1844: 105) D.G.Mann (Round *et al.* 1990: 671) (Table 2).

**TABLE 1.** Primers used for the nested PCR procedure to amplify *rbcL* from single cells.

Primer	Primer sequence (5'–3')	Reference
<i>rbcL</i> 66+ (PCR1)	TTTAAGGAGAAATAAATGTCTCAATCTG	Alverson <i>et al.</i> (2007)
<i>rbcL</i> dP7- (PCR1)	AAASHDCCTTGTGTWAGTVTC	Daugbjerg & Anderson (1997)
<i>rbcL</i> 1444- (PCR2)	GCGAAATCAGCTGTATCTGTWG	Ruch & Theriot (2011)
<i>rbcL</i> 40+ (PCR2)	GGACTCGAATVAAAAGTGAACG	Ruch & Theriot (2011)
Or		
<i>rbcL</i> 1174R (PCR2)	ACCRATTGTACCACCACCRA	This study
<i>rbcL</i> 166F (PCR2)	CAGCTTGTGAYCGYTACCGT	Thus study

**TABLE 2.** Sequence sample data and associated collection numbers for specimens used in this study.

Taxon	CANA #	Genbank #
<i>N. iridis</i>	CANA:128327	MN419022, MN419023
<i>N. fossum</i>	CANA:108598	KP325205, KU674657, KM999089
<i>N. promontorium</i>	CANA:100021, 93416	KU674715, KU674706
<i>N. saccoense</i>	CANA:100021, 93279	KU674689, KU674711
<i>N. bisulcatum</i>	UTEX:FD417	KU674602
<i>N. dilatatum</i>	CANA:108605	KU674654, KU674742
<i>N. potapovae</i>	CANA:108131, 108128	KU674612, KU674597
<i>N. tumescens</i>	CANA:108128	KM999091, KU674596
<i>N. affine</i>	CANA:108613	KU674652, KU674652, KP325202
<i>N. hitchcockii</i>	CANA:100021	KP325181, KU674592
<i>N. amphigomphus</i>	CANA:108124	KP325193, KU674599
<i>N. lowei</i>	CANA:108593, 100021	KU674660, KU674589
<i>N. productum</i>	UTEX:FD116	KU674603, HQ912446
<i>N. longiceps</i>	CANA:108131	HQ912447, KU674629, KU674625
<i>N. vandusenense</i>	CANA: 128327	MN419015, MN419016, MN419017, MN419018, MN419019, MN419020, MN419021
<i>N. collare</i>	CANA: 128327	MN419024
<i>N. lavoieanum</i>	CANA: 128327	MN419025
<i>Neidiomorpha binodis</i>	D168_001	MN238808
<i>Neidiomorpha binodiformis</i>	D168_009	MN238809
<i>Scolioleura peisonis</i>	—	HQ912473
<i>Luticola ventricosa</i>	—	KY86486

Nested PCR amplifications for single cell isolations were performed on partial coding regions of the chloroplast gene *ribulose1, 5-biphosphate carboxylase/oxygenase large subunit (rbcL)* using primers listed in Table 1. Sequencing was completed using the protocol of Hamilton *et al.* (2015) using an AB Applied Biosystems 3100-Avant Genetic analyser (Applied Biosystems, Foster City, California, USA). The sequences were edited in Geneious v. 6.1.5 (Geneious, Newark, New Jersey, USA), and the consensus sequences were aligned using the MAFFT alignment tool with an auto algorithm, scoring matrix 200PAM/K=2, gap penalty 1.53 and offset value 0.123. In this study, the *rbcL* sequences ranged in length from 625 to 1281 base pairs. The program RaxML version 8.2.11 (Stamatakis, 2014) in Geneious version 11.1.5 was used to run a maximum-likelihood (ML) analysis on the *rbcL* alignment. A rapid bootstrapping and search for best scoring ML-tree algorithm was used, with a GTR + I + G nucleotide model, partitioning by codon, and 1000 bootstrap replicates.

## Results

The small stream and Livingstone Lake (pond) in the VanDusen Botanical garden are man-made with annual maintenance activities that create a relatively disturbed aquatic system. The pH of the water in January 2019 was weakly alkaline (pH 7.85) with a moderate specific conductance ( $163.3 \mu\text{S cm}^{-1}$ ) and hardness ( $45.7 \text{ mg L}^{-1}$ ). A detailed water analysis was completed during the cold season (January 24, 2019, Table 3), less than one month after the observation of living cells. Total phosphorus (TP) and total nitrogen (TN) levels were high indicating a meso- to eutrophic water system with TN being the more prominent nutrient (TN:TP >21:1). Ion concentrations of calcium & sodium were the prominent cations with compatible carbonate and sulfate anion concentrations. An ion balance calculations showed that calcium carbonate was predominant followed by sodium chloride. Silica levels as Si were not limiting ( $6.61 \text{ mg L}^{-1}$ ). Iron was the prominent heavy metal, followed by Strontium and Manganese. No metal concentrations (17 in total) identified in the Canadian Guidelines for Aquatic Life were above the identified limits for water quality. Metals below detection limit included Bismuth, Cesium, Cobalt, Lithium, Nickel, Silver, Tellurium, Thallium, Thorium, Tin and Tungsten.

**TABLE 3.** Water chemistry, physical, salts, nutrients and metals for Livingstone Lake (Pond), VanDusen Botanical Garden.

<b>VanDusen Botanical Garden, Livingstone Lake, Channel</b>			
Date Sampled	24-Jan-2019		
Parameter	Detection Limit	Units	Water
Physical Tests (Water)			
Hardness (as CaCO <sub>3</sub> )	0.50	mg L <sup>-1</sup>	45.7
Anions and Nutrients (Water)			
Bromide (Br)	0.050	mg L <sup>-1</sup>	<0.050
Chloride (Cl)	0.50	mg L <sup>-1</sup>	13.8
Fluoride (F)	0.020	mg L <sup>-1</sup>	0.021
Nitrate (as N)	0.0050	mg L <sup>-1</sup>	0.623
Nitrite (as N)	0.0010	mg L <sup>-1</sup>	0.0041
Total Nitrogen	0.030	mg L <sup>-1</sup>	0.963
Phosphorus (P)	0.0020	mg L <sup>-1</sup>	0.0448
Sulfate (SO <sub>4</sub> )	0.30	mg L <sup>-1</sup>	6.57
Total Metals (Water)			
Aluminum (Al)	0.0030	mg L <sup>-1</sup>	0.131
Antimony (Sb)	0.00010	mg L <sup>-1</sup>	0.00022
Arsenic (As)	0.00010	mg L <sup>-1</sup>	0.00332
Barium (Ba)	0.00010	mg L <sup>-1</sup>	0.0228
Beryllium (Be)	0.00010	mg L <sup>-1</sup>	<0.00010
Bismuth (Bi)	0.000050	mg L <sup>-1</sup>	<0.000050
Boron (B)	0.010	mg L <sup>-1</sup>	0.014
Cadmium (Cd)	0.0000050	mg L <sup>-1</sup>	0.0000369
Calcium (Ca)	0.050	mg L <sup>-1</sup>	14.0
Cesium (Cs)	0.000010	mg L <sup>-1</sup>	<0.000010
Chromium (Cr)	0.00010	mg L <sup>-1</sup>	0.00100
Cobalt (Co)	0.00010	mg L <sup>-1</sup>	<0.00010
Copper (Cu)	0.00050	mg L <sup>-1</sup>	0.00210
Iron (Fe)	0.010	mg L <sup>-1</sup>	0.252
Lead (Pb)	0.000050	mg L <sup>-1</sup>	0.000317

.....continued on the next page

TABLE 3. (Continued)

VanDusen Botanical Garden, Livingstone Lake, Channel			
Date Sampled	24-Jan-2019		
Parameter	Detection Limit	Units	Water
Lithium (Li)	0.0010	mg L <sup>-1</sup>	<0.0010
Magnesium (Mg)	0.0050	mg L <sup>-1</sup>	2.61
Manganese (Mn)	0.00010	mg L <sup>-1</sup>	0.0318
Molybdenum (Mo)	0.000050	mg L <sup>-1</sup>	0.000179
Nickel (Ni)	0.00050	mg L <sup>-1</sup>	<0.00050
Phosphorus (TP)	0.050	mg L <sup>-1</sup>	0.056
Selenium (Se)	0.000050	mg L <sup>-1</sup>	0.000060
Silicon (Si)	0.10	mg L <sup>-1</sup>	3.61
Silver (Ag)	0.000010	mg L <sup>-1</sup>	<0.000010
Sodium (Na)	0.050	mg L <sup>-1</sup>	9.13
Strontium (Sr)	0.00020	mg L <sup>-1</sup>	0.0892
Sulfur (S)	0.50	mg L <sup>-1</sup>	2.19
Tellurium (Te)	0.00020	mg L <sup>-1</sup>	<0.00020
Thallium (Tl)	0.000010	mg L <sup>-1</sup>	<0.000010
Thorium (Th)	0.00010	mg L <sup>-1</sup>	<0.00010
Tin (Sn)	0.00010	mg L <sup>-1</sup>	<0.00010
Titanium (Ti)	0.00030	mg L <sup>-1</sup>	0.00536
Tungsten (W)	0.00010	mg L <sup>-1</sup>	<0.00010
Uranium (U)	0.000010	mg L <sup>-1</sup>	0.000013
Vanadium (V)	0.00050	mg L <sup>-1</sup>	0.00069
Zinc (Zn)	0.0030	mg L <sup>-1</sup>	0.0053
Zirconium (Zr)	0.000060	mg L <sup>-1</sup>	0.000075
Qualifier	Hardness was calculated from Total Ca and/or Mg concentrations and may be biased high (dissolved Ca/Mg results unavailable).		

## Species Descriptions

Division Bacillariophyta  
 Subdivision Bacillariophytina  
 Class Bacillariophyceae  
 Order Neidiineae  
 Family Neidiaceae

### *Neidium iridis* (Ehrenb.) Cleve (1894: 69) Fig. 1

Individuals examined for morphology: n = 28, examined for molecular analysis: n = 2.

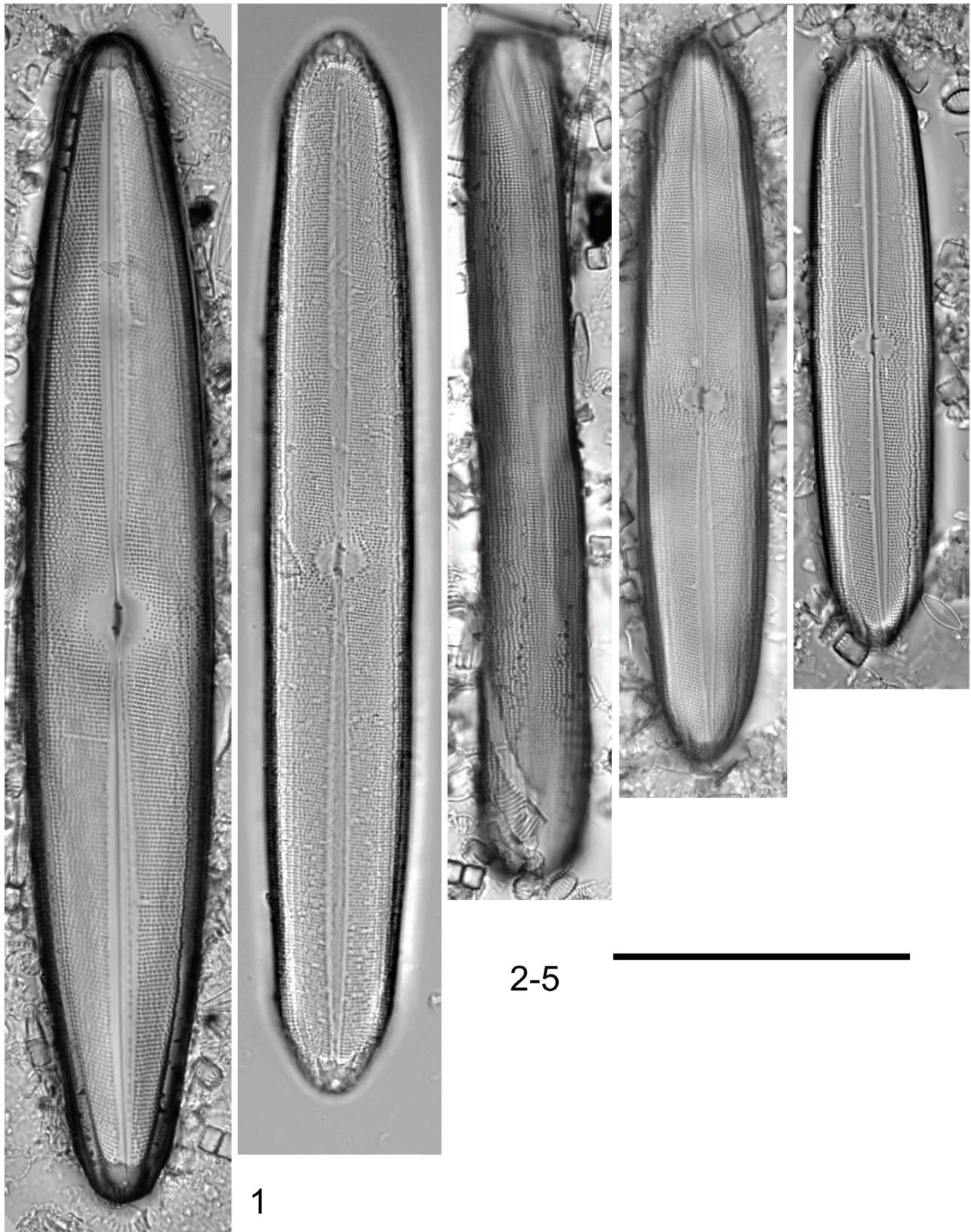
Frustules isovalvar. Valves linear to linear elliptic with narrowing obtuse to sagittate apices. Length 184–275 µm, 20.0–37.5 µm wide, 14–15 striae in 10 µm and 14–15 areolae in 10 µm. One large longitudinal canal present along each margin. Striae parallel at mid-valve, parallel to weakly convergent at apices (Fig. 1). Axial area linear to linear elliptic from center to apex. Central area round to weakly elliptic, covers approximately 1/3–1/2 of mid-region of valve. In LM, raphe lateral with tightly curved proximal raphe ends and terminal fissures end at laciniae.

Observations:—*Neidium iridis* was found from a single locality (multiple samples) collected from VanDusen Botanical Garden, British Columbia, Canada. The species is identified by its plastid *rbcL* DNA sequence, large size relative to other *Neidium* taxa, one longitudinal canal along each margin and the sagittate shape of valve apices.

**TABLE 4. Summary metrics for the *Neidium* taxa examined.**

Taxon	<i>N. affine</i>	<i>N. amphigomphus</i>	<i>N. beanyi</i>	<i>N. bisulcatum</i>	<i>N. collare</i>	<i>N. dilatatum</i>	<i>N. fossium</i>	<i>N. hitchcockii</i>	<i>N. tridis</i>	<i>N. lavoisianum</i>	<i>N. longiceps</i>	<i>N. lowei</i>	<i>N. potapovae</i>	<i>N. productum</i>	<i>N. promontorium</i>	<i>N. sacroense</i>	<i>N. tumescens</i>	<i>N. vandocense</i>
Length (µm)	31–84.5	73–141	126–201	35–75	44–95	174–269	92–142	62–85	184–275	59–70	28–47	78–135	29.5–51.5	60–100	51–85	55–118	181–216	96–116
Width (µm)	10–18	23–38	18–27	7–12	14.5–20	40–55	2.5–34	14–22	20–37.5	14–15	8–12	15–29	7.5–12.5	20–30	14–22	16–35	55–83	20–23
Striae (in 10 µm)	22–28	15–19	15–18	26–30	14–18	16–19	17–21	19–22	14–15	20–22	30–36	20–24	24–30	16–18	20–28	16–22	15–17	14–17
Aeolae (in 10 µm)	20–28	14–20	14–18	24–28	16–19	14–18	17–20	20–24	14–15	15–18	30–36	17–24	24–30	17–20	20–26	16–21	14–18	14–16
Valve outline	linear to linear lanceolate	linear elliptic to linear elliptic lanceolate	Linear elliptic to lanceolate	linear	elliptic-lanceolate lanceolate	elliptic-lanceolate to lanceolate	elliptic-lanceolate	linear	Linear to linear-elliptic	linear to linear-elliptic	Linear	lanceolate, elliptic lanceolate	linear, linear-lanceolate	Linear	linear	linear	broadly lanceolate to elliptical	Linear to linear-elliptic
Central area	ca. rounded, 1/3 to 1/2 valve width	round to elliptical ca. 1/3 valve width	small round, transversally expanded, <1/2 valve width	Transversally elliptic to round	Transversally expanded, <1/2 valve width	transversally 1/2 to 1/3 valve width	transversal, 1/3 to 1/2 valve width	transversal 1/2 to 3/4 valve width	round to weakly elliptic, <1/2 valve width	transversally expanded, 1/2 to 3/4 valve width	broadly linear	Transversally elliptic	Elliptical, >1/2 valve width	Transversally elliptic	Elliptical, 1/3–1/2 valve width	Elliptical, 1/2 valve width	transversally expanded, rounded	Transversally expanded, <1/2 valve width
Central raphe ends	short, curved	small hooks	small deflected hooks	hooked	deflected, long	tightly hooked	hooks	deflected, long forked	tightly curved	deflected, long	deflected	tightly rounded	deflected	deflected	deflected, long	deflected, long	tight hooks	deflected hooks
Striation	Parallel, convergent at apices	parallel to weakly oblique	Parallel, weakly convergent at apices	Parallel to convergent at apices	oblique to midly convergent	weakly radiate to convergent	Parallel, weakly convergent at apices	Parallel	Parallel to weakly convergent	midly oblique throughout	Parallel to slightly convergent at apices	Parallel to weakly convergent at apices	Parallel	Parallel to weakly convergent at apices	Striae parallel, to curved radiate at apices	Parallel to weakly convergent at apices	weakly radiate at center to parallel/convergent at apices	Oblique to weakly convergent at apices
Longitudinal canals	2–3	3–5	>3	1	1	5+	1	1	1	1	1	1	1	1	1	1	>9	>3
Apices	sagittate to rostrate	acute rounded apices	sagittate to cuneate	rounded	rostrate to broad apiculate	narrow pointed apices	subacute	acute, apiculate rounded	sagittate	capitate	subcapitate to capitate	cuneate, rounded	Rostrate	transversal, 1/3 to 1/2 valve width	apiculate to subrostrate	apiculate to subrostrate	narrow rostrate	apiculate extended apices
Reference	Lefebvre et al. 2017	Lefebvre & Hamilton 2015	This study	Patrick & Reimer 1966	This study	Lefebvre & Hamilton 2015	Lefebvre & Hamilton 2015	Lefebvre & Hamilton 2015	This study	This study	Lefebvre et al. 2017	Lefebvre et al. 2017	Lefebvre et al. 2017	Patrick & Reimer 1966	Lefebvre et al. 2017	Lefebvre et al. 2017	Lefebvre & Hamilton 2015	This study

*Neidium iridis* has a large size range (length, 184–275  $\mu\text{m}$ ) in this population which is comparable to *N. iridis* from the type locality and another locality in eastern North America (Hamilton *et al.* 2019). *N. iridis* is comparable to *N. beattyi* but can be distinguished by the valve shape, valve size and number of longitudinal canals.



FIGURES 1–5. *Neidium iridis* (Fig. 1) and *Neidium beattyi* sp. nov. (Figs 2 (holotype), 3–5). Scale bar = 50  $\mu\text{m}$ .

*Neidium beatyi* sp. nov. Figs 2–18

Individuals examined for morphological analyses: n = 48, no molecular material recovered.

Frustules rectangular. Valves linear elliptic to lanceolate with weak sagittate to cuneate apices (Figs 2–5). Valve length 126–201 µm, width 18.0–27.0 µm. Areolae round to elliptical, striae oblique to weakly radiate at apices, 15–18 in 10 µm. Areolae 14–18 in 10 µm. Voigt faults distinct on secondary side of valve. Central area small round to transapically expanded, covering 1/3 to 1/2 the valve width. Axial area linear-elliptical from mid-valve to apex. In LM, raphe filiform and linear-elliptical. Three or more longitudinal canals present along each margin. Central raphe ends small deflected hooks, terminal ends forming bifurcate lacinia. Small terminal hyaline area present at apex. In girdle view, areolae form lineal apical and transapical rows (Fig. 3).

In SEM external view, raphe linear with thickened ridges along each side (Figs 6–8). Ridges terminate prior to apex (Fig. 11). Proximal ends form distinct small hooks in opposite directions on small central mound. Distal raphe ends form lacinia (Figs 6, 11). Lacinia narrow arrowhead shaped with curved expansion at mantle base (Fig. 11). Axial area scattered with surface depressions. Areolae adjacent to axial area orientated towards axial area and not directly up from valve face (Fig. 8). Areolae around central area larger and more linear elliptic randomly scattered. Areolae depressions on external valve face with recessed finger-forming silicate cribra (Figs 7, 9). Areolae chambered with transapical interconnections (Fig. 12). Areolae around central area sometimes larger than valve face areolae. Three to five longitudinal canals present along each valve margin (Figs 8–11). Longitudinal canal flat with valve face (Figs 8, 9). At apex, narrow linear slit-like areolae may open from a longitudinal canal (Figs 10, 11). Internal valve: central area elevated with ghost striae. Helictoglossae linear and interconnected (Fig. 13). Terminal helictoglossae vertical and curl back from terminal nodule (Fig. 14). Longitudinal canals centrally, forming small bulge along valve margin; towards apex one canal extends to hyaline terminal nodule at apex (Figs 14, 15, 17). Longitudinal canals form apical and transapical network of interconnections (Fig. 18). Internally, areolae covered by fine poroid hymenes (Figs 15–17). Renilimbria (2–6) around areolae along axial area, and longitudinal canals (Fig. 16). Renilimbria randomly scattered around areolae on valve face.

Holotype:—CANADA. British Columbia: Vancouver, VanDusen Botanical Garden, J. Holmes, December 28, 2016. Small stream at the end of Livingstone Lake (pond) (CANA! 126257-2, fig. 2 holotype specimen circled on slide. Isotype ANSP GC65328 (circled specimen on slide). Genbank# No DNA results).

Etymology:—The specific epithet (*beatyi*), is linked to the generosity of the Beaty Foundation in supporting the Beaty Botanical Museum, the VanDusen Botanical Garden and the Canadian Museum of Nature.

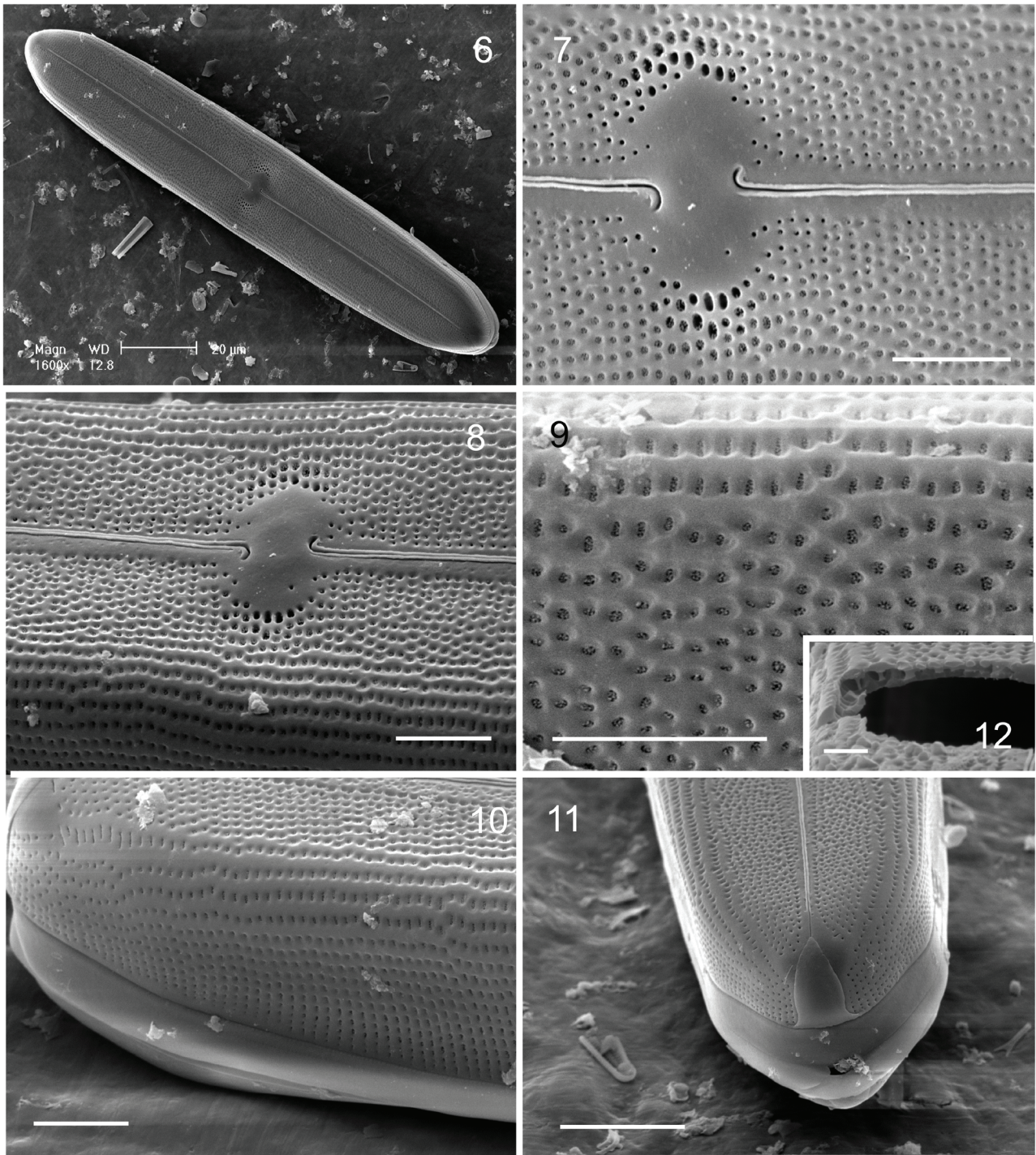
Registration: <http://phycobank.org/102929>

Observations:—*Neidium beatyi* was found from a regional locality (multiple samples) collected from VanDusen Botanical Garden, British Columbia, Canada. The species is identified by its size, 3–6 longitudinal canals and shape of valve including apices. *Neidium beatyi* has a large size range (length, 126–207 µm) and is similar to *Neidium subampliatum* (Grunow) Flower (2005: 54). Flower (2005) elevated the taxon *Navicula firma* var. *subampliatum* Grunow. (Schmidt 1877, 49: 19) [note: as a typing mistake *Neidium firma* var. *subampliatum*] to the rank of species within the genus *Neidium*. For *N. subampliatum* he chose a neotype, since a holotype specimen was not available. *Neidium subampliatum* (specimens) presented by Flower (2005, p. 64, 51–55) are significantly smaller than *N. beatyi*, with one longitudinal canal and the shape form is different (Supplement A). However, the valve morphology of *N. subampliatum* sensu Flower does not represent the original line drawing of *Navicula firma* var. *subampliatum*, which is larger relative to other taxa on Schmidt's original plate. Further, Kobayashi (1968) illustrated a specimen he identified as *Neidium iridis* var. *subampliatum* (Grun.) Kobayashi (1968: 102) from the vicinity of Tokyo that is similar to our specimens and the line drawing of Schmidt for *N. firma* var. *subampliatum*.

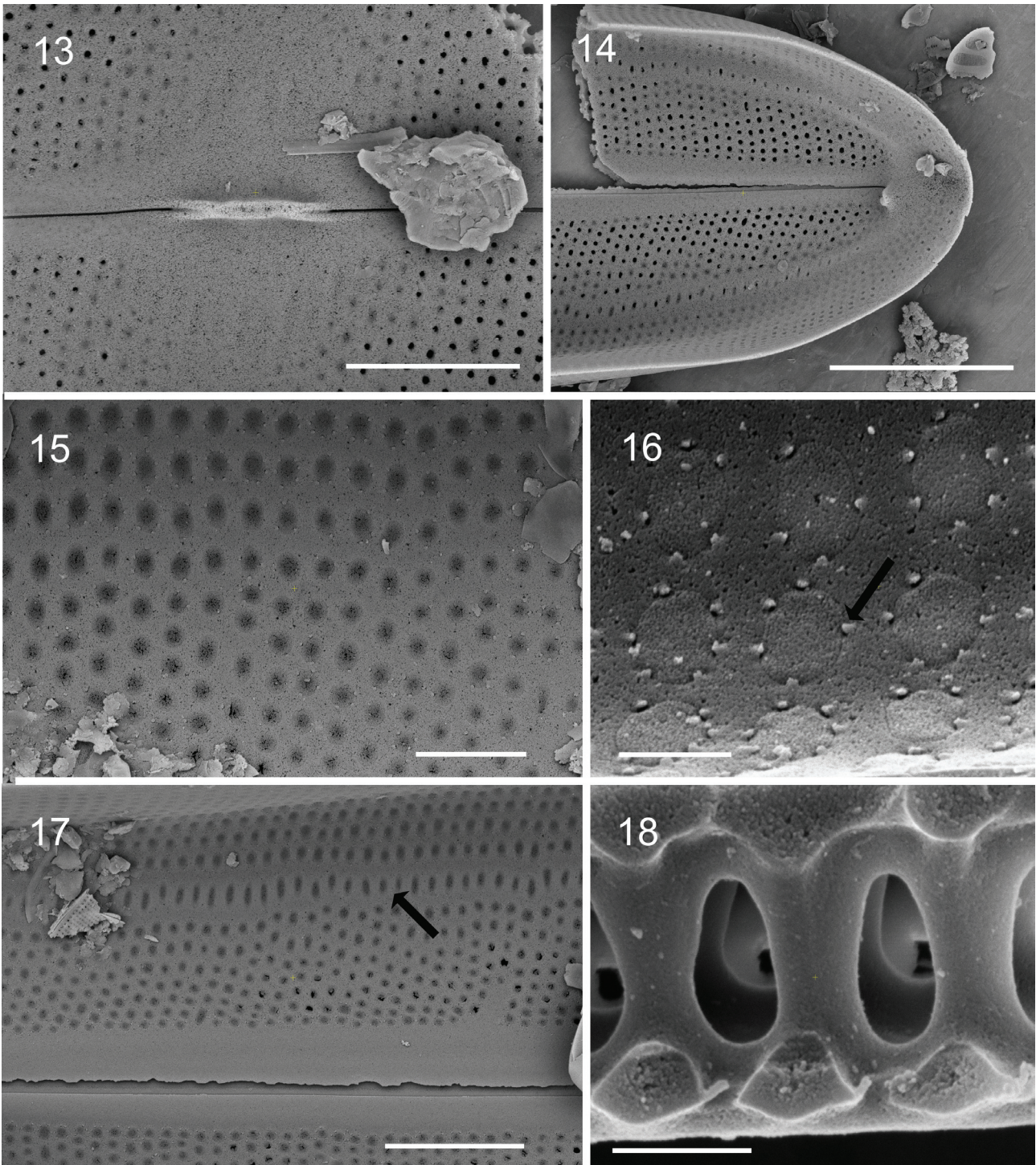
*Neidium reimeri* John (1981: 571–572) and *N. zoigaeum* Liu *et al.* (2017: 17) are similar, but are smaller in size (both taxa <115 µm) and the apices of these taxa are weakly cuneate to round, not notably drawn out, cuneate to sagittate. In addition, the formation of the proximal helictoglossae seems to differ (connected together in *N. beatyi*). It is possible that *N. reimeri* and *N. zoigaeum* are simply smaller populations of *N. beatyi* with some loss of valve form with smaller sizes. Both genetic and more thorough morphological studies of these taxa are required.

*Neidium iridis* is similar in valve shape and was also found at the same locality, although rare. *Neidium reimeri* is distinguished by size (*N. iridis* 184–237 µm long, 32–25 µm wide), number of longitudinal canals (3–5 versus 1 canal in *N. iridis*), higher stria count and the presence of an elevated ridge adjacent to the raphe. *Neidium iridis* sensu auct. (Metzeltin & Lange-Bertalot 2007) is similar in valve shape form, with multiple longitudinal canals, but this South American form is much larger (ca. 300 µm long) and requires more study. *Neidium cuneatum* Krammer & Metzeltin (= *N. iridis*; Metzeltin & Lange-Bertalot, 1998: 146, pl. 124: 6) also has a similar valve outline, but is larger (>196 µm long), only one longitudinal canal and has fewer striae. See Hamilton *et al.* (2019) for a more complete discussion of *N.*

*iridis* including *N. maximum* (Cleve 1894: 69) Meister (1912: 109). The large size of *N. beatyi* and valve shape can also be compared with *N. obliquestriatum* (Schmidt 1877: figs 49: 41, 42) Cleve (1894: 69), but distinguished by shape, number and size of longitudinal canals (1 for *N. obliquestriatum*), size and formation of the proximal raphe ends, round to transapically elongated central area (*N. beatyi*) and shape of the apices. Also comparable is *N. krasskei* Metzeltin & Lange-Bertalot (2007: 174–175) which is <103 µm long. *Neidium beatyi* is larger, apices are not as cuneate and central raphe ends smaller. No SEM images of *N. krasskei* are available for comparison.



**FIGURES 6–12.** *Neidium beatyi* sp. nov. SEM, external view. **Fig. 6.** Whole valve. **Fig. 7.** Central area raphe with silica ridges along each side. **Figs 8, 10.** Valve margin and mantle with multiple longitudinal canals. Copulae 2 rows of poroids. **Fig 9, 12.** Recessed areolae chambered and interconnected with finger-like cribra. **Fig. 11.** Apex showing arrow-like bifurcate lacinia. Copulae (3 evident) open bands with no evident poroids. Scale bars = 20 µm: Fig. 6; 10 µm: Fig. 11; 5 µm: Figs 7–10; 2 µm: Fig. 12.



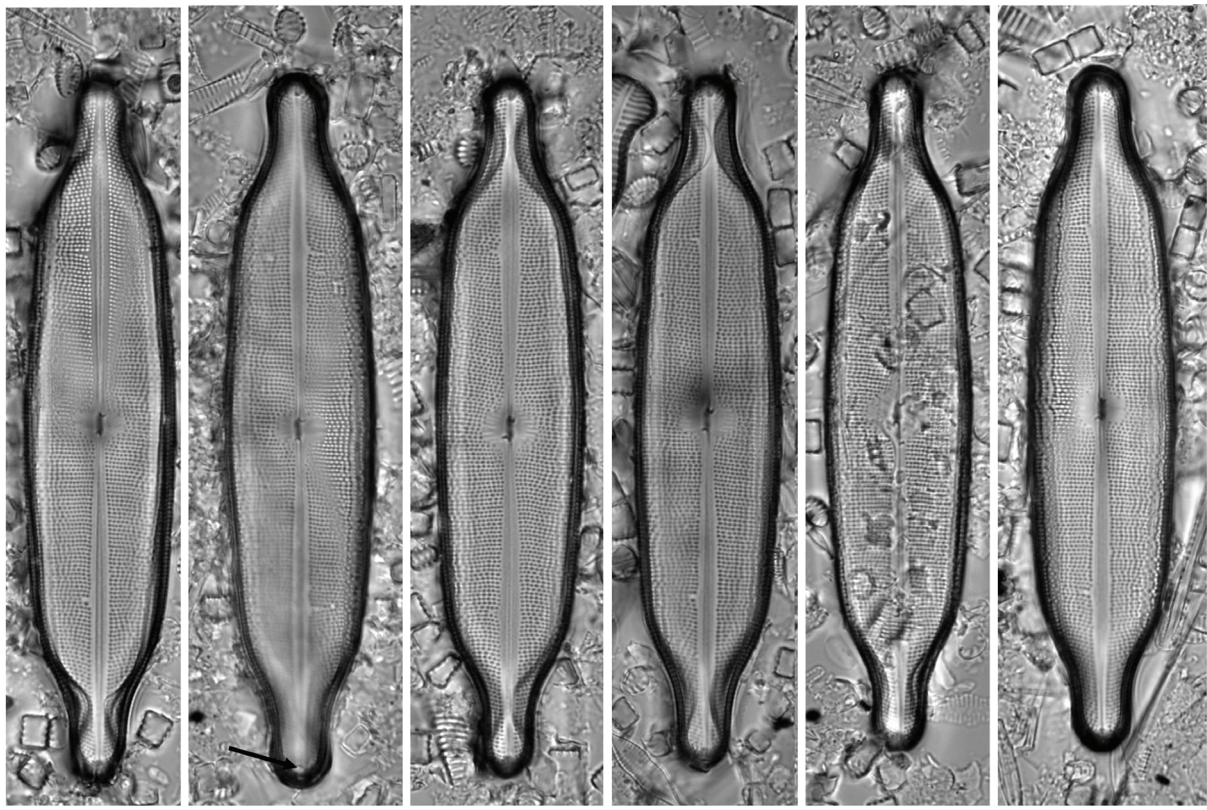
**FIGURES 13–18.** *Neidium beatyi* sp. nov. SEM internal view. **Fig. 13.** Central area with linear forming interconnected helictoglossae. **Fig. 14.** Apex with a curved forming helictoglossa at the edge of the terminal nodule. A single prominent longitudinal canal extends to the nodule. **Figs 15, 17.** Multiple longitudinal canals; at center canal similar (Fig. 15), towards apex one becomes more prominent (Fig. 17, arrow). **Fig. 16.** Renilimbria surround hymenae covered areolae (arrow). **Fig. 18.** Open chambered formation (apically and transapically) of the longitudinal canal. Scale bars = 10  $\mu$ m: Fig. 14; 5  $\mu$ m: Figs 13, 17; 2  $\mu$ m: Fig. 15; 500 nm: Figs 16, 18.

*Neidium vandusenense* sp. nov. **Figs 19–44**

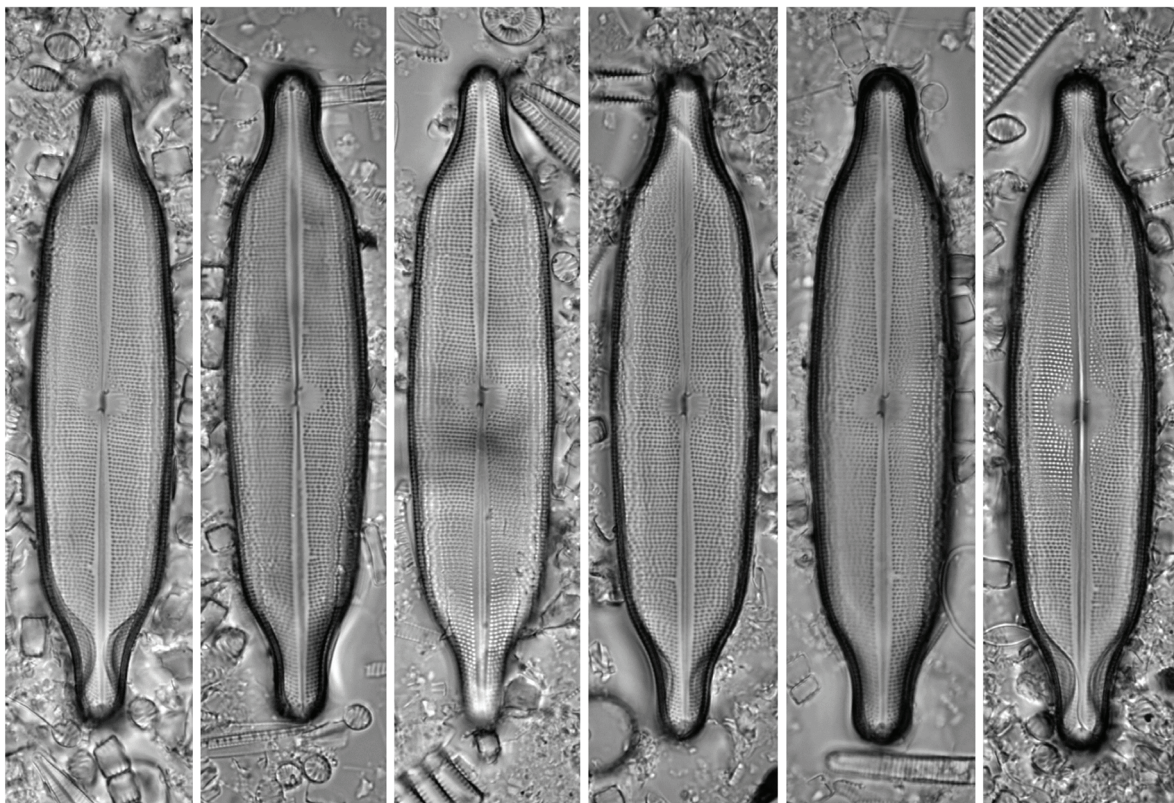
Individuals examined for morphological analyses: n = 61, examined for molecular analysis: n = 7.

Valves linear to linear elliptic with apiculate extended apices (Figs 19–30). Valve length 96–116  $\mu$ m, width 20.0–23.0  $\mu$ m. Striae oblique to mildly convergent at apices, 14–17 in 10  $\mu$ m. Areolae round to elliptical, 14–16 in 10  $\mu$ m. Voigt faults on secondary side of valve. Central area transapically expanded, covering 1/3 to 1/2 the valve width.

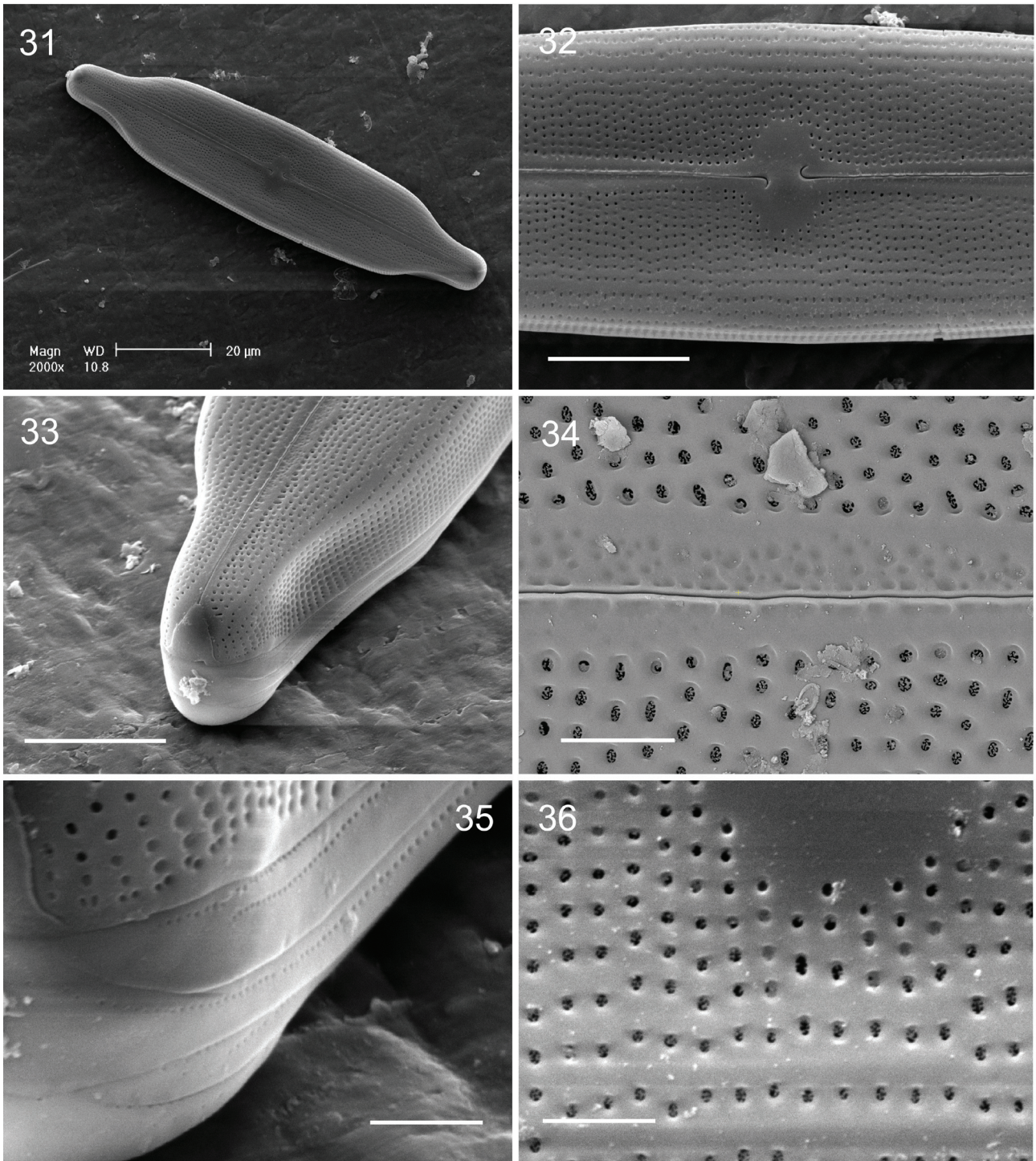
Linear ghost striation markings present along edge of central area (Figs 21–22, 25, 27–28). Axial area linear-elliptical from mid-valve to apex. In LM, raphe filiform and linear-elliptical. Three or more longitudinal canals present along each margin. Central raphe ends deflected hooks, terminal ends forming bifurcate lacinia. Small terminal hyaline area present at apex (Fig. 20, arrow).



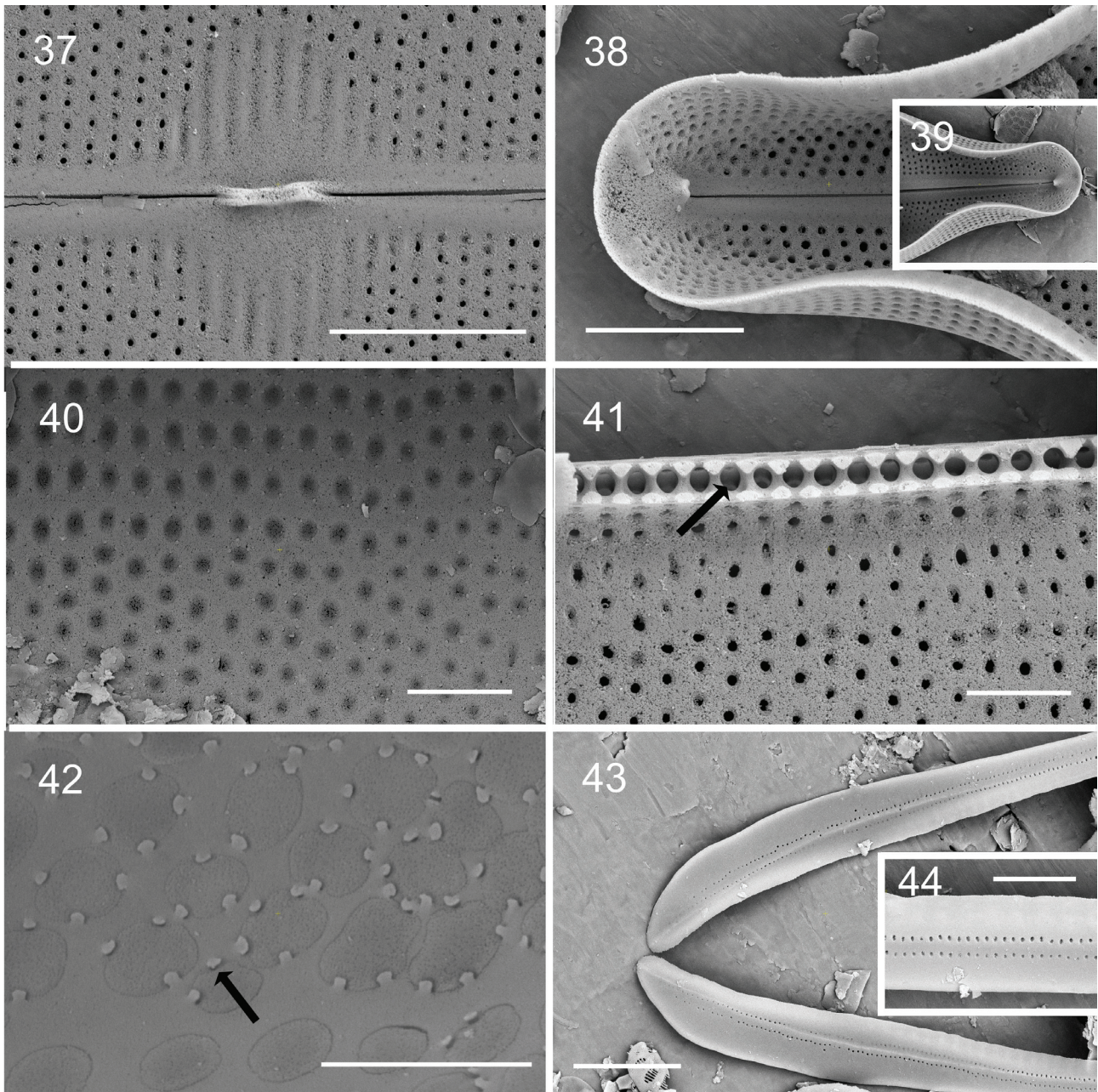
19-30



**FIGURES 19–30.** *Neidium vandusenense* sp. nov. LM. Fig. 21, holotype. Scale bar = 20  $\mu$ m.



**FIGURES 31–36.** *Neidium vandusenense* sp. nov. SEM, external view. **Fig. 31.** Whole valve. **Fig. 32.** Central valve with multiple longitudinal canals and transapical central area. Proximal raphe branches evenly hooked. **Fig. 33.** Apex valve face and mantle showing concave mantle wall, longitudinal canals reducing to one at the apex. **Fig. 34.** Valve face showing developed ridge along one side of the raphe (arrow) and scattered surface depressions along the axial area. Areolae recessed with a finger-like cribra. **Fig. 35.** Apex with 3 evident copulae. Copulae open bands with 2 rows of pores. Lacina extends to band base (arrow). **Fig. 36.** Central region showing a weak elevation of the longitudinal canal. Scale bars = 20 µm: Fig. 31; 10 µm: Figs 32, 33; 2 µm: Figs 34–36.



**FIGURES 37–44.** *Neidium vandusenense* sp. nov. SEM, internal view. **Fig. 37.** Central area with offset forming interconnected helictoglossae. Surface depressions (ghost striae) present in the central area. **Figs 38, 39.** Apex showing upright formation of the helictoglossae at the edge of the terminal nodule. Longitudinal canals blend in with areolae. **Figs 40, 41.** Margin of the valve showing multiple longitudinal canals. Open chambered formation (Fig. 41 (arrow), apical and transapical). **Fig. 42.** Renilimbic surround hymenae covered areolae (arrow). **Figs 43, 44.** Open copula band with 2 rows of poroids. Scale bars = 5  $\mu$ m: Figs. 37, 38, 43; 2  $\mu$ m: Figs 40, 41; 1  $\mu$ m: Figs 42, 44.

In SEM external view, valves more or less linear with rounded margins (Figs 31, 33). Apices broadly protracted and mantle at apex recessed not forming linear sides (Figs 31, 33). Raphe linear with a broken thickened ridge along primary side and weak to no ridge along secondary side (Figs 32, 34). Proximal raphe ends form distinct small hooks in opposite directions on small central mound (Fig. 32). Distal raphe ends form broad triangular lacinia with curved expansion at mantle base (Figs 33, 35). Axial area with randomly positioned surface depressions (Figs 32, 34). Areolae depressions on external valve face with recessed finger-forming silicate cribra (Figs 34, 36). Three to four flat, longitudinal canals present along each margin (Figs 32, 36). Internal valve: Central area elevated with ghost striae (Fig. 37). Central helictoglossae offset with small silica interconnection. Terminal helictoglossae form vertically on terminal

nodule (Figs 38, 39). Canals flat with valve face, all of equal size and form (Figs 40, 41); towards apex canals extends to hyaline terminal nodule at apex (Fig. 38). Areolae chambered with transapical interconnections (Fig. 41 arrow, on mantle). Areolae covered by hymenes (Figs 42, 43). Renilimbria (2–6) around areolae along axial area, and longitudinal canals (Fig. 42). Renilimbria also randomly scattered around areolae on the valve face. Copulae open bands, with 2 rows of pores (Figs 43, 44).

Type:—CANADA. British Columbia: Vancouver, VanDusen Botanical Garden, J. Holmes, December 28, 2016. Small stream at the end of Livingstone Lake (pond) (holotype: CANA! 126257-7, fig. 22 holotype specimen, circled on slide). Isotype ANSP GC65327 (circled specimen on slide). Genbank #s See table 2.

Etymology:—The specific epithet (*vandusenense*), is recognized for the collection site at the VanDusen Botanical Garden.

Registration: <http://phycobank.org/102030>

Observations:—Plastid *rbcL* DNA sequence, size (96–116 µm), valve outline, 3–4 longitudinal canals, ghost striae along the margins of the central area and recessed mantle margins at the apices identify this taxon. *Neidium vandusenense* can be compared to *N. siveri* Metzeltin & Lange-Bertalot (2007: 179) with a similar valve outline, but *N. vandusenense* is distinguished by the larger size (64–74 µm long, *N. siveri*), more than one longitudinal canal and the weak oblique striation formation.

*Neidium vandusenense* can also be compared to *N. grande* Gandhi (1959: 313, as *N. grandis*) with respect to general valve outline, protracted apices, and multiple longitudinal canals. *N. vandusenense* is differentiated from *N. grande* by larger size (45–55 µm, *N. grande*), linear to slightly triundulate valve margins (not elliptic), and stria density (26–28 in 10 µm, *N. grande*). No ghost striae were observed in *N. grande*. Another comparison can be made with *N. capitellatum* Gandhi (1959: 313, as *N. capitellata*) with respect to valve outline, although *N. capitellatum* is smaller (46–86 µm long) and the apices are capitate.

In North America compare with *N. affine* var. *humerus* Reimer (Patrick & Reimer 1966: 392) with respect to similar valve outline and ghost striae along the central area. *N. vandusenense* is larger than *N. affine* var. *humerus* (41–78 µm long), the valve margins of *N. vandusenense* are more linear and sometimes weakly triundulate, the apices more protracted and 3+ longitudinal canals versus 1(2) in *N. affine* var. *humerus*. The stria and areolae densities of *N. affine* var. *humerus* are also higher.

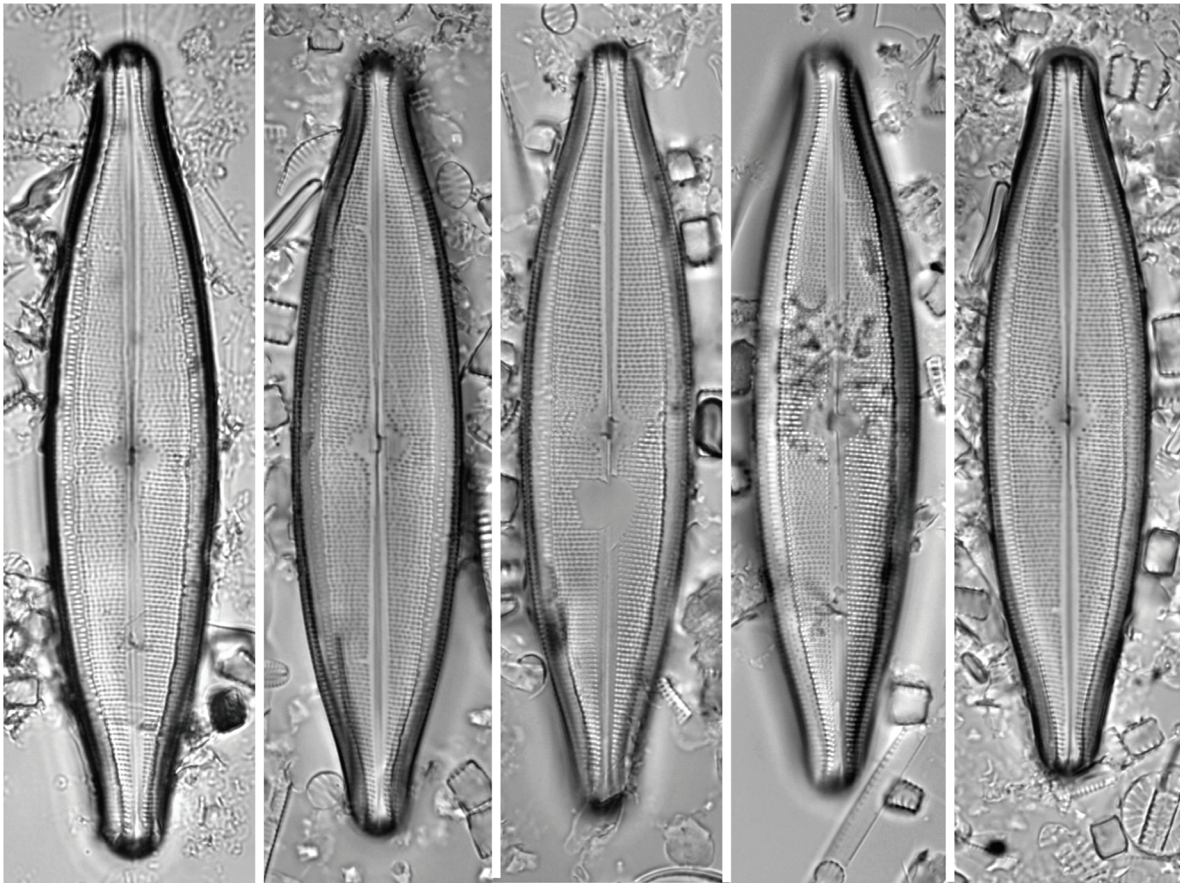
#### *Neidium collare* sp. nov. Figs 45–68

Individuals examined for morphological analyses: n = 31, examined for molecular analysis: n = 1.

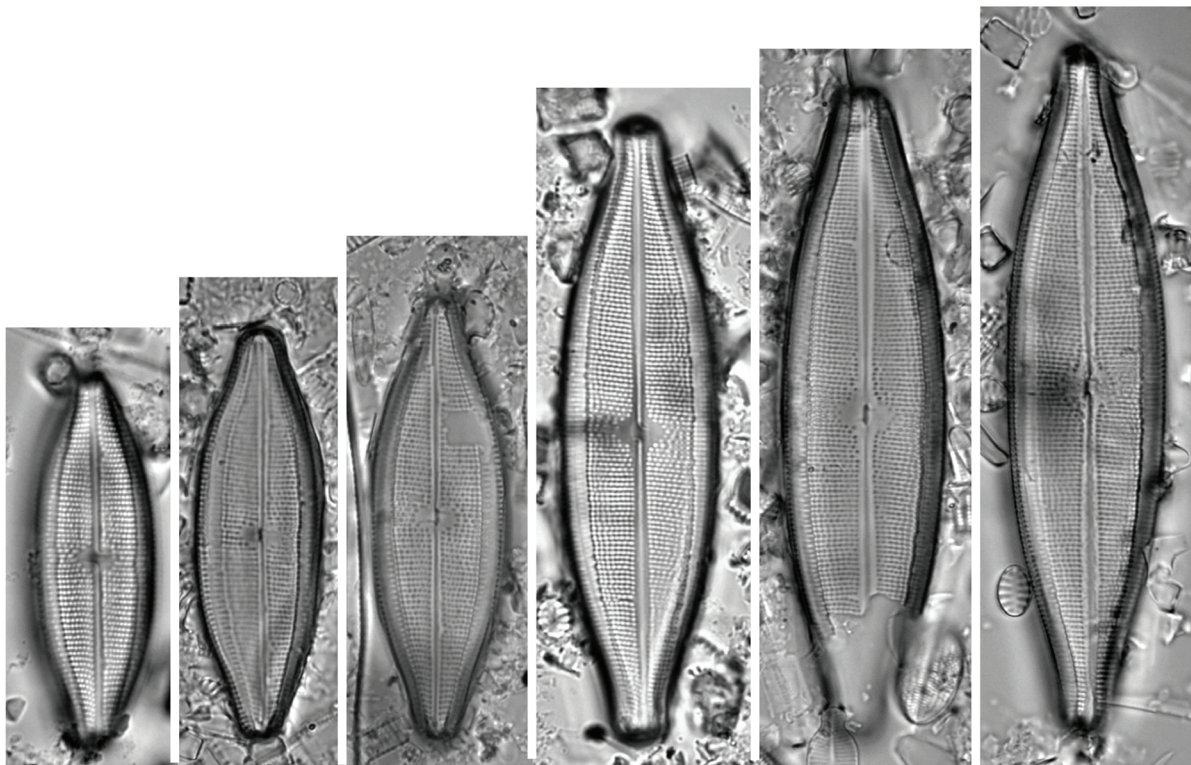
Valves elliptic lanceolate to lanceolate with rostrate to broadly apiculate apices (Figs 45–55). Valve length 44–96 µm, width 14.5–20.0 µm. Striae oblique to mildly convergent at apices, 14–18 in 10 µm. Areolae round to elliptical, 16–19 in 10 µm. Voigt faults on secondary side of valve. Central area transapically expanded, covering 1/3 to 1/2 valve width. Axial area linear from mid-valve to apex. In LM, raphe filiform and linear-elliptical. One large longitudinal canal present along each margin. Central raphe ends deflected extending 1/2 to 3/4 across central area. Terminal ends forming bifurcate lacinia.

In SEM external view, raphe linear, curving to secondary side of valve close to apex (Figs 56, 60, 61). Proximal raphe ends deflected, not hooked on small central mound (Fig. 57). Distal raphe ends form a small triangular lacinia (Figs 60, 61). Axial area straight to linear-elliptic with no surface depressions (Figs 56, 57). One longitudinal canal along each margin with a single row or linear elliptic areolae (Fig. 58). Areolae round to elliptic with no cribra formation evident (Fig. 59). One round to elliptic areola opening from the longitudinal canals all the way to the apex. (Figs 60, 61). Copulae open bands with two rows of pores (Figs, 58, 60, 61). Internal valve: Central area elevated with weak ghost striae. Central helictoglossae offset with silica interconnection (Figs 62, 65, 66). Terminal helictoglossae forms vertically (not recurved) at edge of small terminal nodule (Fig. 64). Canal along each margin elevated from valve face, extending from apex to apex with a single row of linear elliptic areolae (Figs 63, 64, 67). Areolae opening recessed from valve face and covered by hymenes (Fig. 67). Areolae chambered with transapical interconnections (Fig. 68, on mantle). Renilimbria around areolae along axial area, and longitudinal canals. Renilimbria also randomly scattered around areolae on the valve face (Fig. 66, arrows).

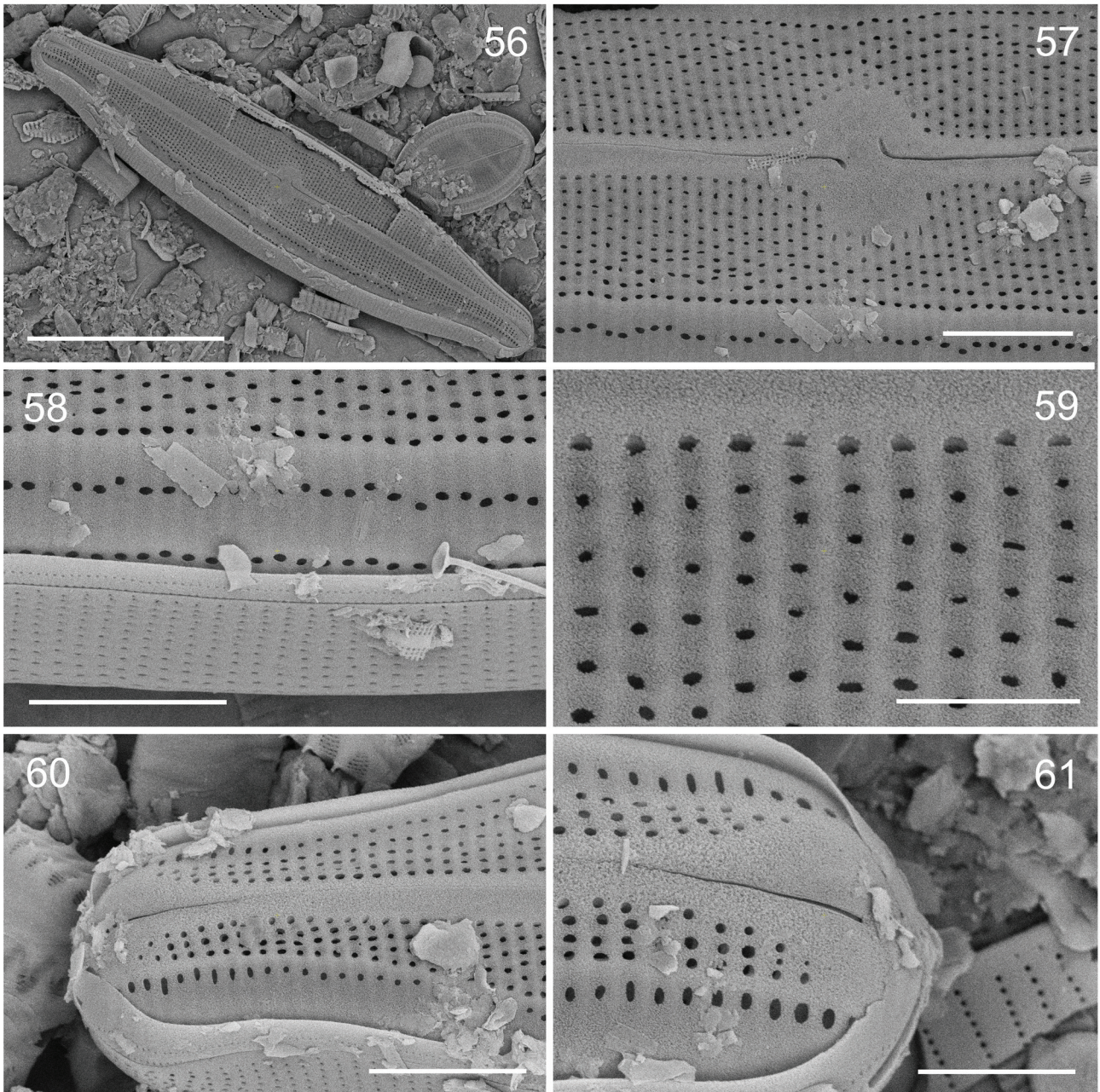
Type:—CANADA. British Columbia: Vancouver, VanDusen Botanical Garden, J. Holmes, December 28, 2016. Small stream at the end of Livingstone Lake (pond) (holotype: CANA! 126257-4, fig. 49 holotype specimen, circled on slide). Isotype ANSP GC65326 (specimen circled on slide). Genbank # See Table 2.



45-55



FIGURES 45–55. *Neidium collare* sp. nov. LM. Fig. 49, holotype. Scale bar = 20  $\mu$ m.



**FIGURES 56–61.** *Neidium collare* sp. nov. SEM, external view. **Fig. 56.** Whole valve. **Fig. 57.** Central valve with longitudinal canal and transapical central area. Proximal raphe branches deflected. **Fig. 58.** Valve face mantle junction with epivalve, hypovalve and copula band. **Fig. 59.** Valve face with developed areolae. Areolae without finger-like cribra. **Fig. 60.** Apex with open bands of copulae. Copulae with 2 rows of pores. Lacinia weakly developed. **Fig. 61.** Apex showing no apparent lacinia. Longitudinal canals extend to the tip of the apex. Scale bars = 30  $\mu\text{m}$ : Fig. 56; 5  $\mu\text{m}$ : Figs 57, 58, 60; 3  $\mu\text{m}$ : Fig. 61; 2  $\mu\text{m}$ : Fig. 59.

Etymology:—The specific epithet (*collare*), refers to the narrow neck of the valve approaching the apices.

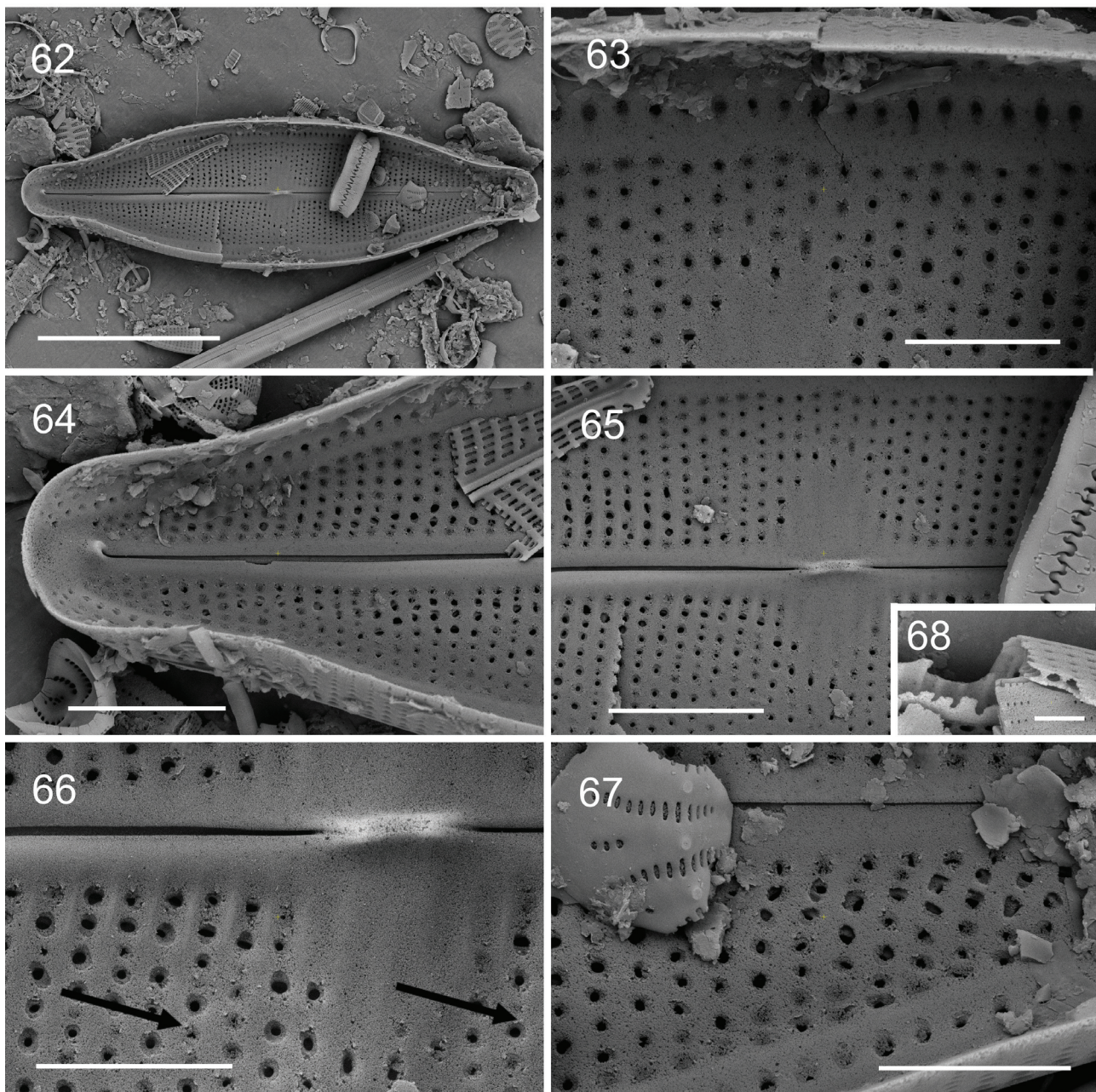
Registration: <http://phycobank.org/102031>

Observations:—The elliptic lanceolate valve form with rostrate to apiculate rounded apices is represented in a number of *Neidium* species. Plastid *rbcL* DNA sequence, size (47–92  $\mu\text{m}$  long), valve outline, one prominent longitudinal canal, weak to no ghost striae along the margins of the central area and formation of the proximal helictoglossae identifies this taxon. *Neidium collare* can be compared with *N. ligulatum* Liu *et al.* (2017: 22) and *N. affine* var. *amphirhynchus* (Ehrenberg 1843: 417) Cleve (1894: 68) sensu Liu *et al.* (2017: 22, figs 204, 207, 216–220). There is a continuum of shape changes from narrowing apiculate (*N. collare*) to rostrate apices (*N. affine* var. *amphirhynchus* sensu Liu *et al.*). Both of these comparable taxa have two clear helictoglossae at the central nodule while, *N. collare* has a merged helictoglossae formation. The distal helictoglossae are vertically projected against the terminal nodule in

*N. collare*, while *N. ligulatum* and *N. affine* var. *amphirhynchus* sensu Liu *et al.* have recurved helictoglossae. *Neidium ligulatum* is at the smaller end of the size spectrum (47–64 µm long) with a slightly lower stria count (14–18 in 10 µm), while *N. affine* var. *amphirhynchus* sensu Liu *et al.* has a slightly higher stria count (18–20 in 10 µm). Genetic studies are required to delineate the relationship between these taxa.

*Neidium collare* can also be compared to *N. oblique-striatum* var. *nipponicum* Skvortzow (1936: 30, as var. *nipponica*) and *N. oblique-striatum* var. *rostratum* Skvortzow (1936: 30, as var. *rostrata*). The Skvortzow taxa have distinct oblique striations with rostrate and sagittate apices. *N. oblique-striatum* var. *nipponicum* is much broader (20–25 µm wide) and *N. oblique-striatum* var. *rostratum* has a higher stria count (24 in 10 µm). The single line drawing limits the understanding of the phenotype expression of these taxa.

In North America, *N. collare* can be compared with the smaller (36–53 µm) *N. statuarium* Siver & Hamilton (2005: p. 364) although *N. collare* has a lower stria count, more lanceolate valve and no extensive valve surface sculpture.

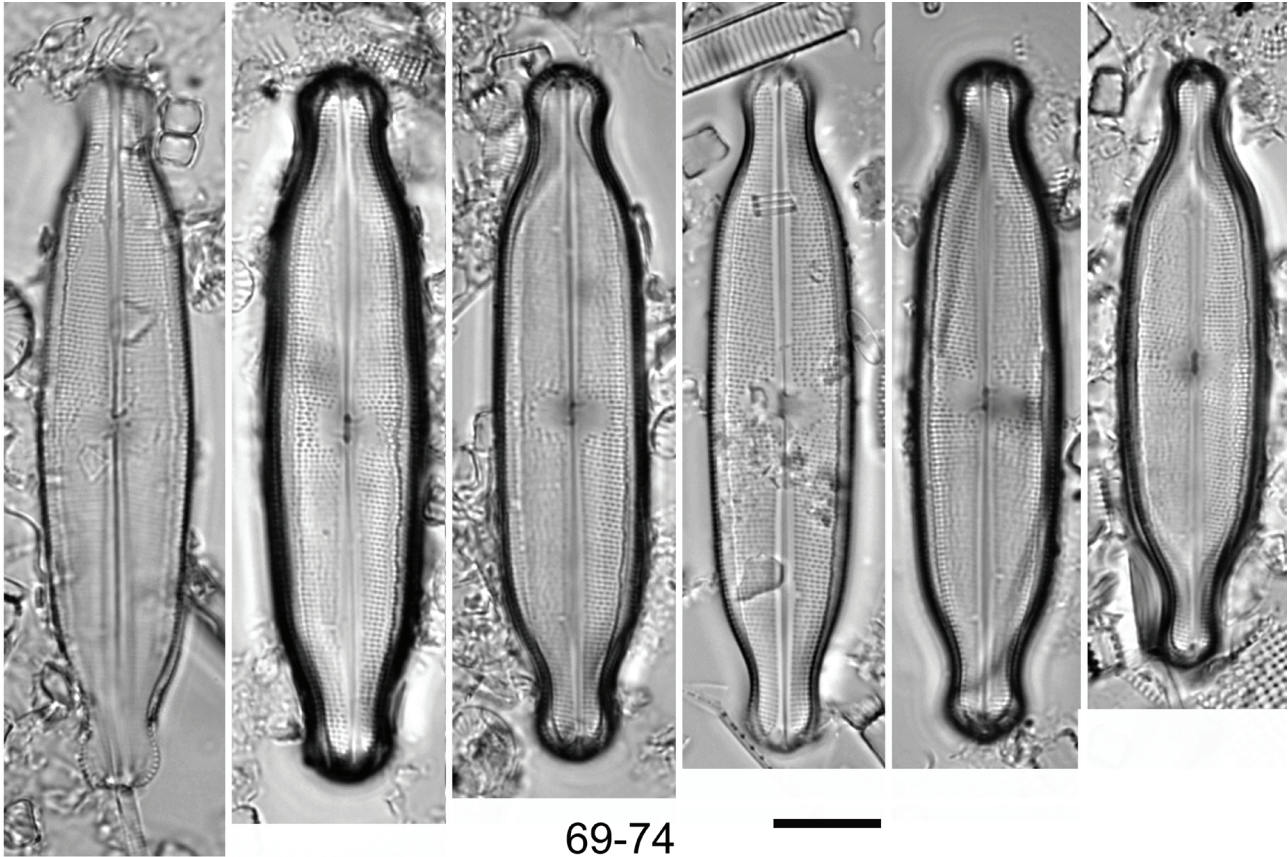


**FIGURES 62–68.** *Neidium collare* sp. nov. SEM, internal view. **Fig. 62.** Whole valve. **Figs 63, 67.** Recessed areolae and longitudinal canals at mid-valve and close to apex. **Figs 65, 66.** Central area with offset forming interconnected helictoglossae. Very weak surface depressions (ghost striae) present in the central area. Remnants of renilimbria present (arrows). **Fig. 64.** Apex showing an erect helictoglossa at terminal nodule and single longitudinal canal extending to the apex. **Fig. 68.** broken valve showing the canal. Scale bars: 20 µm: Fig. 62; 5 µm: Figs 64, 65; 3 µm: Figs 63, 66, 67; 1 µm: Figs 68.

*Neidium lavoieanum* sp. nov. Figs 69–82

Individuals examined for morphological analyses: n = 27, examined for molecular analysis: n = 1.

Valves linear to linear-elliptic with capitate apices (Figs 69–74). Valve length 58–70 µm, width 14–15.0 µm. Striae mildly oblique throughout, 20–22 in 10 µm. Areolae elliptical, 15–18 in 10 µm. Voigt faults on secondary side of valve. Central area transapically expanded, covering  $\frac{1}{2}$  to  $\frac{3}{4}$  valve width. Axial area linear to linear elliptic from mid-valve to apex. In LM, raphe filiform and linear-elliptical. One longitudinal canal present along each margin. Central raphe ends deflected extending  $\frac{1}{2}$  to  $\frac{3}{4}$  across central area. Terminal ends forming bifurcate lacinia.



FIGURES 69–74. *Neidium lavoieanum* sp. nov. LM. Fig. 71, holotype. Scale bar = 10 µm.

In SEM external view, proximal raphe ends deflected and hooked on small central mound (Fig. 77). Raphe with small thickened ridges mid-way across valve. Distal raphe ends form small triangular lacinia extending to base of mantle (Fig. 78). Axial area straight to linear-elliptic with no surface depressions (Fig. 76). One longitudinal canal along each margin, extending to base of terminal raphe fissure (Fig. 78). Longitudinal canal with two external pores, one on valve face, one on mantle (Fig. 75). Areolae round to elliptical, no cribra occlusions evident. Internal view, helictoglossae at raphe ends not, deflected up, not recurved (Figs 79, 81, 82). Terminal apex without prominent pseudosepta (Fig. 82). Central helictoglossae separate, in linear alignment (Fig. 81). Central area broad with recessed coverings between virgae. Areolae chambered (Fig. 80). Areolae openings round to linear-elliptic, covered by hymenae (Fig. 80, arrow). Renilimbria scattered, primarily around longitudinal canals and axial area (Figs 81, 82). Longitudinal canal with single row of elliptical areolae covered with hymenae.

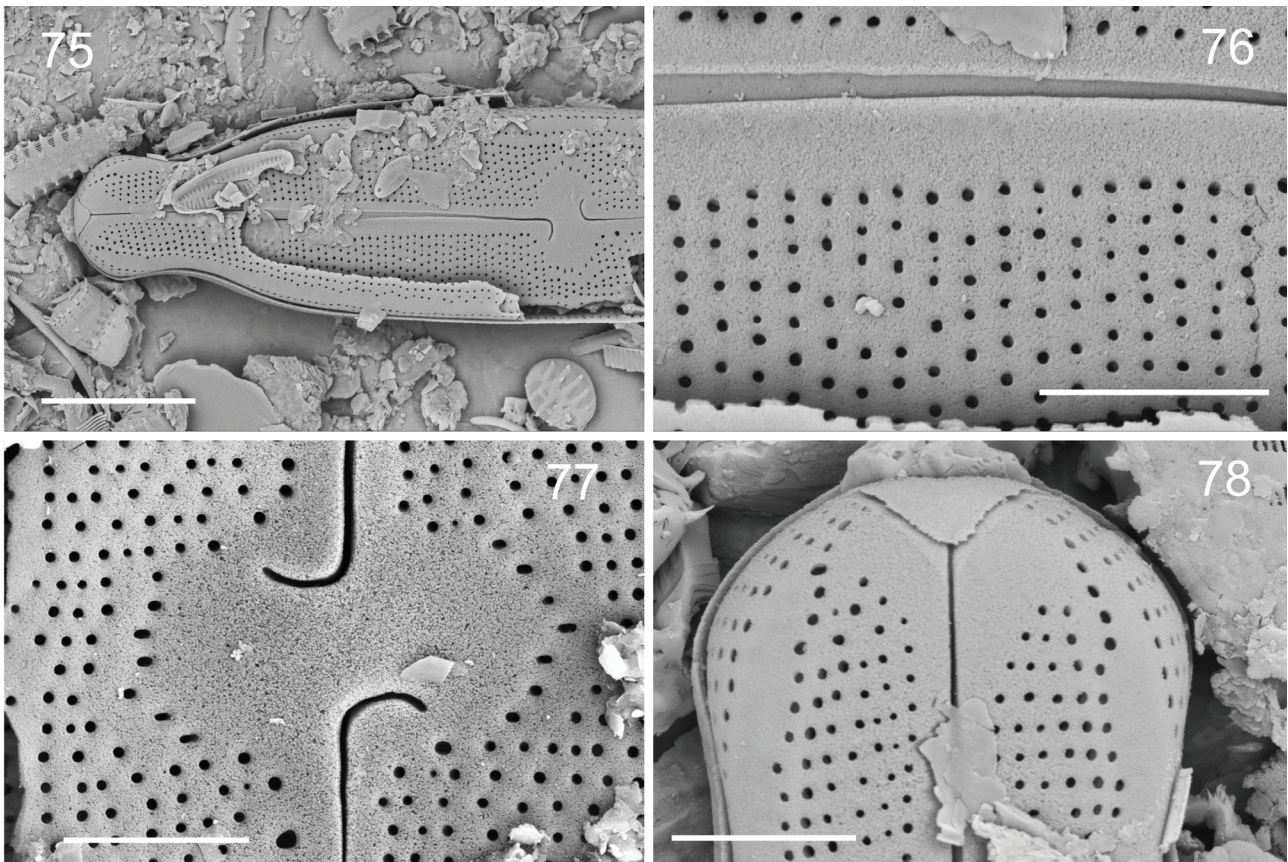
Type:—CANADA. British Columbia: Vancouver, VanDusen Botanical Garden, J. Holmes, December 28, 2016. Small stream at the end of Livingstone Lake (pond) (holotype: CANA! 126257-1, fig. 71 holotype specimen circled on slide.). Isotype ANSP GC65329 (circled specimen on slide). Genbank # See table 2.

Etymology:—The specific epithet (*lavoieanum*) is presented in honour of Dr. I. Lavoie for her exceptional work on ecosystem modelling, diatom ecology, toxicology and teratology.

Registration: <http://phycobank.org/102032>

Observations:—The linear to linear-elliptic valve form with capitate apices is represented in a number of *Neidium* species. At present plastid *rbcL* DNA sequence, size (59–70 µm long), one prominent longitudinal canal, and formation of the proximal helictoglossae identifies this taxon. *Neidium lavoieanum* can be compared with *N. longiceps* (W.Greg.

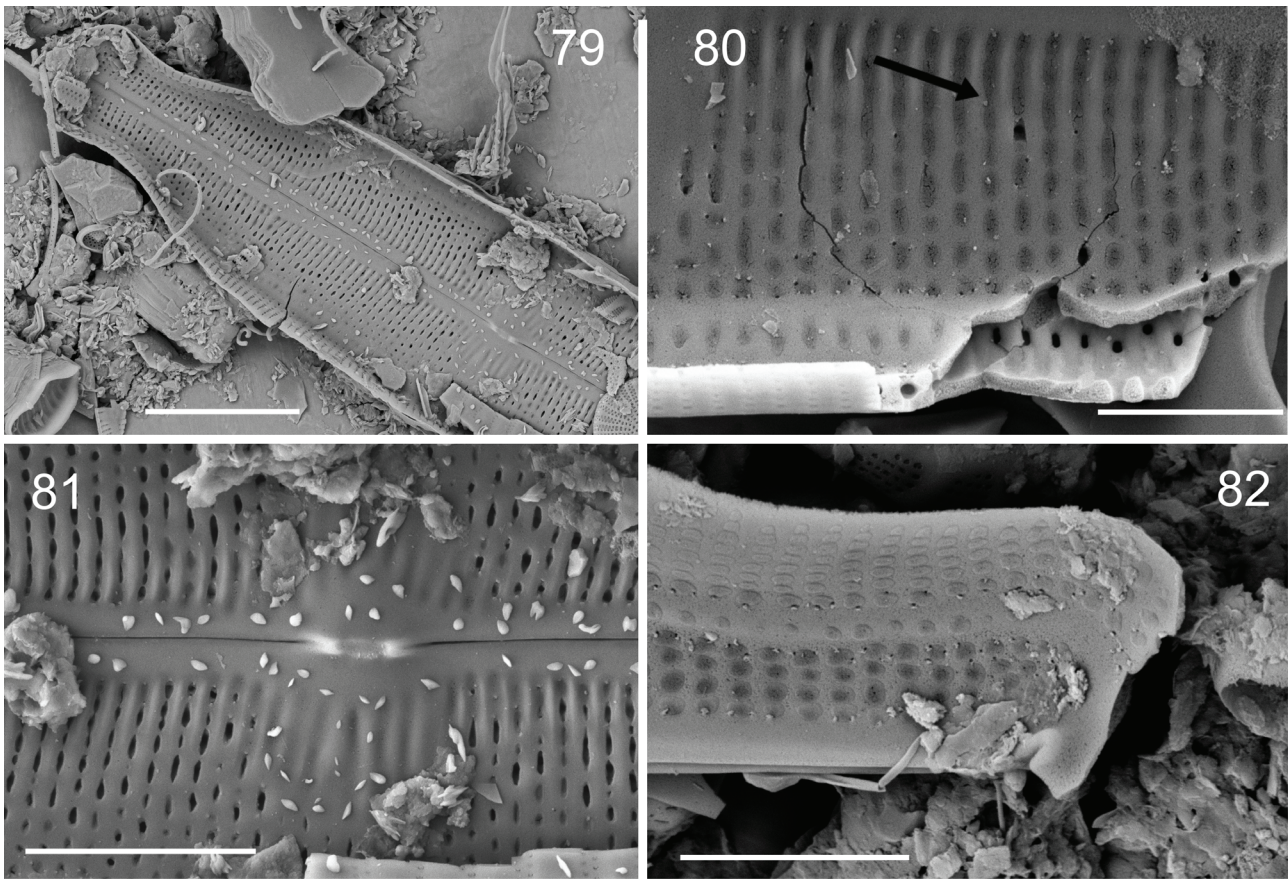
1856: 8) R.Ross (1947: 210) from North America (Lefebvre *et al.* 2017), but separated by larger size (*N. longiceps* 28–47  $\mu\text{m}$  long, 8–12  $\mu\text{m}$  wide), and lower stria count (*N. longiceps* 30–36 in 10  $\mu\text{m}$ ), and a distinct difference in the *rbcL* gene. All other morphological features are similar between the two taxa. Another similar taxon is *N. angustatum* Liu *et al.* (2017: 11), but *N. angustatum* is narrower (10–11  $\mu\text{m}$ ), with a higher stria count (25–27 in 10  $\mu\text{m}$ ), different striae orientation and the apices are more rostrate than capitate. No DNA metrics are available for comparison.



**FIGURES 75–78.** *Neidium lavoieanum* sp. nov. SEM, external view. **Fig. 75.** Half valve. **Fig. 76.** Surface areolae with no occlusions and axial area mid-way along the valve. **Fig. 77.** Elevated central area with elongated areolae along the margin and recurved proximal raphe endings. **Fig. 78.** Apex showing lacinia and longitudinal canals extending to the apex. Scale bars = 10  $\mu\text{m}$ : Fig. 75; 3  $\mu\text{m}$ : Figs 76–78.

#### Genetic Analysis

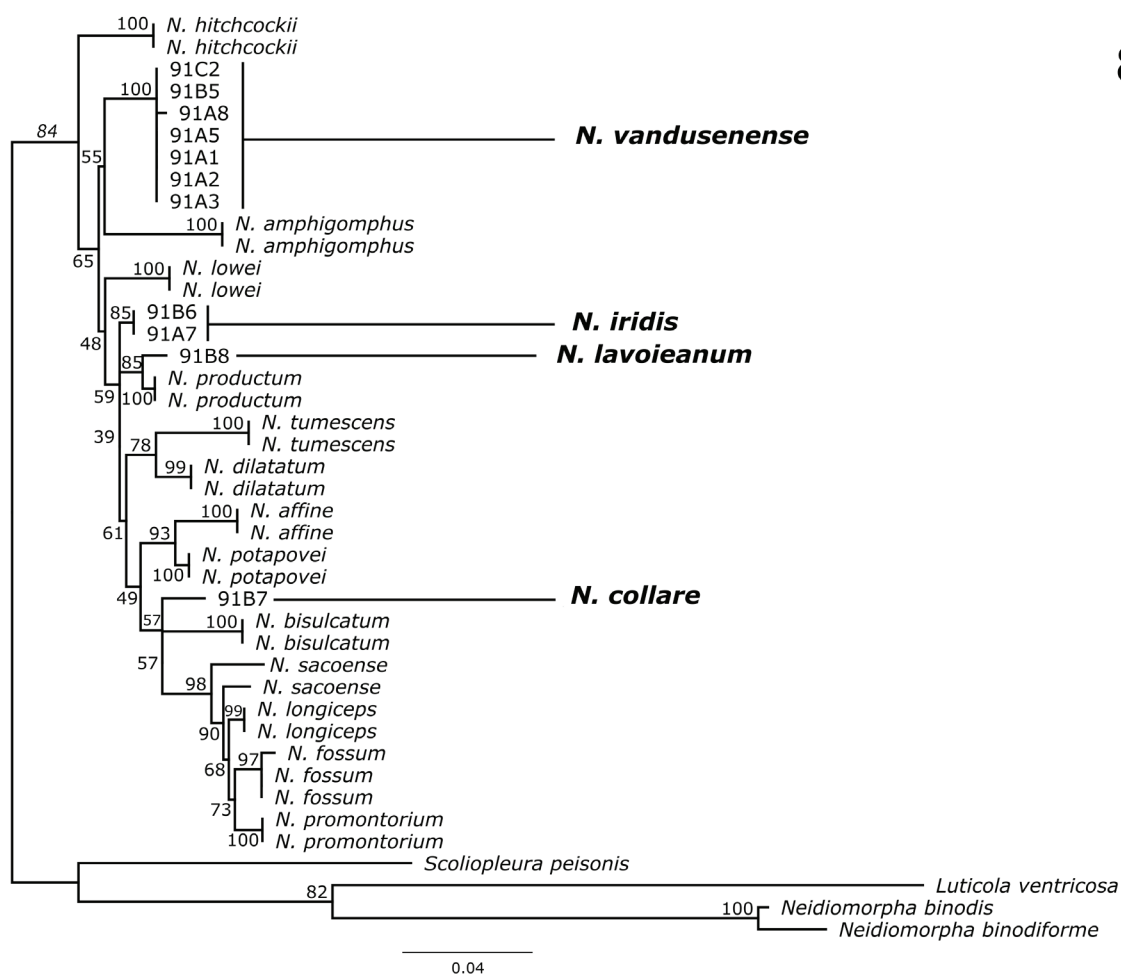
The maximum-likelihood (ML) analyses of *rbcL* sequence data present a broad taxonomic tree across the genus *Neidium* (Fig. 83, Supplement B). Interestingly, the *rbcL* genetic divergence among the *Neidium* taxa examined was relatively low (<1%), however the genetically identified clades separate well with morphology, indicating that *rbcL* is conserved among taxa of this genus. The new species described here were between 0.4 to 0.96% different from their nearest neighbour. For example, *Neidium collare* (n=1) was 0.96% (6 bp different over 625 bp) different from *N. bisulcatum* (Lagerst. 1873: 31) Cleve (1894: 68). *Neidium lavoieanum* was separated from *N. cf. productum* (W.Sm. 1853: 51) Cleve (1894: 69) (Czarnecki culture, UTEX collection) with the smallest difference, 0.40% (3 bp over 751 bp). *Neidium iridis* was also present in the creek sample (Lake Victoria, VanDusen Botanical Garden) and was 0.67% different (5 bp over 750 bp) from *N. lavoieanum*. These differences are in line with established *Neidium* species, for example *N. fossum* and *N. longiceps* are 0.51% different (6 bp over 1168 bp). In the ML analysis, the genus *Neidium* was monophyletic relative to the outgroup taxa included (*Neidiomorpha*, *Luticola* and *Scoliopleura*) and had medium bootstrap support (84%, Fig. 83). *Neidiomorpha binodis* and *N. binodeformis* were associated with *Luticola ventricosa* and sister to *Scoliopleura peisonis*. Within the genus *Neidium*, *N. hitchcockii* was sister to the other species included in this study. A clade including *N. fossum* Lefebvre & P.B.Hamil. (2015, 214), *N. longiceps*, *N. saccoense* Reimer (1959: 29) (Patrick & Reimer 1966: 402, pl 37: 3), and *N. promontorium* Lefebvre & P.B.Hamil. (2017: 696, 697) had high support (98%), while many of the other relationships between species were poorly supported in this analysis (Fig. 83).



**FIGURES 79–82.** *Neidium lavoieanum* sp. nov. SEM, internal view. **Fig. 79.** Half valve showing valve outline. **Fig. 80.** Broken longitudinal canal with areolae and internal valve face areolae. Arrow indicates renilimbria. **Fig. 81.** Internal central nodule with a covering over the verminae along the margin. Helictoglossae separated and aligned. **Fig. 82.** Apex, showing longitudinal canal extending to the apex and an erect helictoglossa next to hyaline thickened apex. Scale bars = 10  $\mu$ m: Fig. 79; 5  $\mu$ m: Fig. 81; 3  $\mu$ m: Figs 80, 82.

## Discussion

Genetic studies on specimens from the genus *Neidium* can show discrimination of taxa when valve structure and shape form are problematic in identifications (e.g. *N. collare* and *N. promontorium*). In contrast, some taxa have distinct valve morphologies with genetically low divergence values (<1%, compared to other taxa) using *rbcL* sequences (e.g. *N. vandusenense* and *N. amphigomphus*). It is evident that genetic and morphological metrics in combination will be required to identify species and ultimately the phylogeny of the genus *Neidium*. *Neidium hitchcockii* is presently the most distinct taxon based on morphology and nuclear and plastid DNA sequence data (Lefebvre & Hamilton 2015, Lefebvre *et al.* 2017). We hypothesized that longitudinal canal formation (specifically number) would be integral in subgeneric evolutionary processes linked to the importance of locomotion in diatom evolution (Nakov *et al.* 2018). With the limited number of taxa available for genetic study, it appears that number and complexity of the longitudinal canal formation taxa may separate out (at least in part) selected taxa in the genetic tree (Fig. 83). The presence of a single marginal longitudinal canal was evident in one clade of the tree (taxa including *N. collare*, *N. bisulcatum*, *N. saccoense*, *N. fossum*, *N. promontorium*, *N. longiceps*), while two or more canals were in another clade (taxa including *N. potapovae* Lefebvre *et al.* (2017: 693, 694) and *N. affine* (Ehrenb. 1843: 417) Pfitzer (1871: 39)). Likewise, taxa with multiple canals, *N. amphigomphus* and *N. vandusenense* in a clade and *N. tumescens* (Grun. in Schmidt 1877: 70) Cleve (1894: 70), and *N. dilatatum* (Ehrenb. 1843: 418) Cleve (1894: 70) in another were evident. However, other taxa with single canals like *N. lowei*, *N. productum*, *N. lavoieanum* and *N. iridis* were not clearly associated with clades and highlight that available data is limiting.



**FIGURES 83.** RaxML phylogenetic tree construction showing bootstrap (BS) confidence levels using the gene *rbcL* for selected taxa within the genus *Neidium*.

The complexity of the longitudinal canals including valve wall formation (degree of chamber development) may become more relevant in future analyses. Other factors like surface ornamentation and occlusions (present or not) may also be of future importance. The significance of renilimbria to the genus *Neidium* is poorly understood. However, Siver (pers. comm.) and P. Hamilton (pers. obs.) suspect that renilimbria are holding the structure of the cytoplasmic membrane primarily around the axial area and longitudinal canals as part of the locomotion process. Presently, the cribra formation over the external opening of the areolae does not appear to be significant in subgeneric relationships.

The biogeographic distribution of *Neidium* taxa is poorly understood. This is in part due to low abundance of taxa in selected environments and in identifying species with a limited knowledge of phenotypic expression among taxa and more specifically populations. It is evident that South America, North America, Asia and possibly a section of Europe have a broad spectrum of taxa. Our current understanding of the diversity of valve forms does not indicate common radiation events and development of species flocks, with the possible exception of South America. Furthermore water chemistry is driving the occurrence of specific taxa. *Neidium kozlowii* for example is found in the European Alps, North American alpine environments, Mongolian/Asian highlands and the Arctic under moderately alkaline conditions. Also, *N. alpinum* (including *N. alpinum* var. *quadripunctatum*) for example is found in Europe and North America under distinct acidophilic conditions (Hamilton *et al.* 1990). The relationship between environment and biogeographic distributions can certainly be resolved with better data sets and a more complete understanding of phenotypic and genotypic traits in taxa. For example, better documentation of phenotypic expression could show that taxa within the *N. beatyi* mix are one species with biogeographically different degrees of variability. Further, taxa like *N. fossum* or *N. dilatatum*, with a wide distribution across North America, may be important in resolving these questions.

In this study, five taxa were observed from the VanDusen Botanical Garden at a small stream locality (*N. iridis*, *N. beatyi*, *N. collare*, *N. lavoieanum* and *N. vandusenense*). Populations of these taxa were morphologically and

genetically distinct and easily separated. The two large taxa (*N. beatyi* and *N. iridis*) present in the stream were not common and surprisingly not closely associated based on morphological features and valve shape. The complexity of longitudinal canal formation may be the reason for this differentiation. *Neidium beatyi* has morphological similarities with other taxa from Asia, Australia and South America suggesting that these large linear species with multiple canals may be closely related. The current (but limited) evidence suggests that this valve form is geographically widespread in multiple taxa (possibly parallel evolution of shape form?) or that shape forms within a taxon are more variable than currently suspected.

## Disclosure statement

The authors confirm and report no conflict of interest in this research.

## Acknowledgments

The authors wish to thank Joe Holmes and Keely Lefebvre for collecting samples from the VanDusen Botanical Garden. Further, Joe Holmes flagged some unidentified specimens that were later recognized by the authors as *N. iridis* and four new species. Anonymous reviewers further improved this research through ideas, helpful suggestions and criticisms. This project was funded by a Canadian RAC grant to PBH from the Canadian Museum of Nature and by the Federal Ministry of Education and Research [German Barcode of Life 2 Diatoms (GBOL2), grant number 01LI1501E]. We also wish to thank Wolf-Henning Kusber for validation of species epithets.

## References

- Abarca, N., Jahn, R., Zimmermann, J. & Enke, N. (2014) Does the cosmopolitan diatom *Gomphonema parvulum* (Kützing) Kützing have a biogeography? *PLoS ONE* 9: e86885.  
<https://doi.org/10.1371/journal.pone.0086885>
- Cantonati, M., Lange-Bertalot, H. & Angeli, N. (2010) *Neidiomorpha* gen. nov. (Bacillariophyta): A new freshwater diatom genus separated from *Neidium* Pfitzer. *Botanical Studies* 51: 195–202.
- Cleve, P.T. (1894) Synopsis of the Naviculoid diatoms. *Kongliga Svenska Vetenskaps Akademiens Handlingar* 26 (2): 1–194.  
<https://doi.org/10.5962/bhl.title.54740>
- Cox, E.J. (1996) *Identification of Freshwater Diatoms from living Material*. Chapman & Hall, London, 158 pp.
- Darriba, D., Taboada, G.L., Doallo, R. & Posada, D. (2012) jModelTest 2: more models, new heuristics and parallel computing. *Nature Methods* 9 (8): 772.  
<https://doi.org/10.1038/nmeth.2109>
- Droege, G., Barker, K., Astrin, J., Bartels, P., Butler, C., Cantrill, D., Coddington, J., Forest, F., Gemeinholzer, B., Hobern, D., Mackenzie-Dodds, J., Ó Tuama, É., Petersen, G., Sanjur, O., Schindel, D. & Seberg, O. (2014) The Global Genome Biodiversity Network (GGBN) Data Portal. *Nucleic Acids Research* 42 (D1): D607–D612.  
<https://doi.org/10.1093/nar/gkt928>
- Ehrenberg, C.G. (1840) Charakteristik von 274 neuen Arten von Infusorien. *Bericht über die zur Bekanntmachung geeigneten Verhandlungen der Königlich-Preussischen Akademie der Wissenschaften zu Berlin* 1840: 197–219.
- Ehrenberg, C.G. (1843) Verbreitung und Einfluss des mikroskopischen Lebens in Süd- und Nord-Amerika. *Abhandlungen der Königl. Akademie der Wissenschaften Zu Berlin* 1841: 291–446.
- Felsenstein, J. (1985) Confidence limits on phylogenies: An approach using the bootstrap. *Evolution* 39 (4): 783–791.  
<https://doi.org/10.1111/j.1558-5646.1985.tb00420.x>
- Flower, R.J. (2005) A taxonomic and ecological study of diatoms from freshwater habitats in the Falkland Islands, South Atlantic. *Diatom Research* 20 (1): 23–96.  
<https://doi.org/10.1080/0269249X.2005.9705620>
- Gandhi, H.P. (1959) Fresh-water diatoms from Sagar in the Mysore State. *Journal of the Indian Botanical Society* 38 (3): 305–331.
- Gregory, W. (1856) Notice of some new species of British fresh-water Diatomaceae. *Quarterly Journal of Microscopical Science* (new

series) 4: 1–14, pl. I.

- Griffith, J.W. (1856) Diatomaceae. In: Griffith, J.W. & Henfrey, A. (Eds.) *The Micrographic Dictionary*. J.V. Voorst, London. First Edition
- Grunow, A. (1860) Über neue oder ungenügend gekannte Algen. Erste Folge, Diatomeen, Familie Naviculaceen. *Verhandlungen der Kaiserlich-Königlichen Zoologisch-Botanischen Gesellschaft in Wien* 10: 503–582, Tabs III–VII.
- Grunow, A. (1878) Algen und Diatomaceen aus dem Kaspischen Meer. In: Schneider, O. (Ed.) *Naturwissenschaftliche Beiträge zur Kenntniss der Kaukasusländer, auf Grund seiner Sammelbeute*. Dresden, pp. 98–132, pls 3–4.
- Hamilton, P.B. & Jahn, R. (2005) Typification of *Navicula affinis* Ehrenberg: Type for the name of the genus *Neidium* Pfitzer. *Diatom Research* 20 (2): 281–294.  
<https://doi.org/10.1080/0269249X.2005.9705637>
- Hamilton, P.B., Lefebvre, K.E. & Bull, R.D. (2015) Single cell PCR amplification of diatoms using fresh and preserved samples. *Frontiers in Microbiology* 6: 1084.  
<https://doi.org/10.3389/fmicb.2015.01084>
- Hamilton, P.B., Poulin, M. & Taylor, M. (1990) *Neidium alpinum* var. *quadripunctatum* (Hustedt) comb. nov., an important acidobiontic taxon from northeastern North America. *Diatom Research* 5: 289–299.  
<https://doi.org/10.1080/0269249X.1990.9705120>
- Hamilton, P.B., Poulin, M. & Walker, D. (1995) *Neidium hitchcockii* (Ehrenberg) Cleve, a morphologically complex taxon within the genus *Neidium* (Naviculales Bacillariophyta). In: Kociolek, J.P. & Sullivan, M.J. (Eds.) *A Century of Diatom Research in North America: a Tribute to the Distinguished Careers of Charles W. Reimer and Ruth Patrick*. Koeltz Scientific Books, Champaign, pp. 66–77.
- Hamilton, P.B., Stachura-Suchoples, K., Kusber, W.-H., Bouchard, A. & Jahn, J. (2019) Typification of the puzzling diatom species *Neidium iridis* (Neidiaceae). *Plant Ecology and Evolution* 152: 392–401.  
<https://doi.org/10.5091/plecevo.2019.1601>
- Huelsenbeck, J.P. & Ronquist, F. (2001) MRBAYES: Bayesian inference of phylogenetic trees. *Bioinformatics (Oxford, England)* 17 (8): 754–755.  
<https://doi.org/10.1093/bioinformatics/17.8.754>
- John, J. (1981) New species of freshwater diatoms from Western Australia. *Nova Hedwigia* 34: 569–576.
- Kobayahi, H. (1968) A survey of the fresh water diatoms in the vicinity of Tokyo. *Japanese Journal of Botany* 20 (1): 93–122.
- Krammer, K. & Lange-Bertalot, H. (1985) Naviculaceae, Neue und wenig bekannte Taxa, neue Kombinationen und Synonyme sowie Bemerkungen zu einigen Gattungen. *Bibliotheca Diatomologica* 9: 1–230.
- Krammer, K. & Lange-Bertalot, H. (1986) Bacillariophyceae. 1. Teil: Naviculaceae. In: Ettl, H., Gerloff, J., Heynig, H. & Mollenhauer, D. (Eds.) *Süßwasserflora von Mitteleuropa* (begründet von A. Pascher) 2/1. Gustav Fischer, Stuttgart, 876 pp.
- Kützing, F.T. (1844) *Die Kieselschaligen*. Bacillarien oder Diatomeen. Nordhausen, 152 pp., 30 pls.  
<https://doi.org/10.5962/bhl.title.64360>
- Lagerstedt, N.G.W. (1873) Sötvattens-Diatomeer från Spetsbergen och Beeren Eiland. *Bihang till Kongliga Svenska Vetenskaps-Akademiens Handlingar* 1 (14): 1–52.
- Lefebvre, K.E. & Hamilton, P.B. (2015) Morphology and molecular studies on large *Neidium* species (Bacillariophyta) of North America, including an examination of Ehrenberg's types. *Phytotaxa* 220 (3): 201–223.  
<https://doi.org/10.11646/phytotaxa.220.3.1>
- Lefebvre, K., Hamilton, P.B. & Pick, F.R. (2017) A comparison of molecular markers and morphology from *Neidium* taxa (Bacillariophyta) from eastern North America. *Journal of Phycology* 53: 680–702.  
<https://doi.org/10.1111/jpy.12537>
- Liu, Q., Kociolek, J.P., Li, B., You, Q. & Wang, Q. (2017) The diatom genus *Neidium* Pfitzer (Bacillariophyceae) from Zoigê wetland, China. Morphology, taxonomy, descriptions. *Bibliotheca Diatomologica* 63: 1–120.
- Mann, D.G. (1984) Auxospore formation and development in *Neidium* (Bacillariophyta). *British Phycological Journal* 19 (4): 319–331.  
<https://doi.org/10.1080/00071618400650371>
- Mann, D.G. (2010) Discovering diatom species: is a long history of disagreements about species-level taxonomy now at an end? *Plant Ecology and Evolution* 143 (3): 251–264.  
<https://doi.org/10.5091/plecevo.2010.405>
- Meister, F. (1912) Die Kiesialgen der Schweiz. In: *Beiträge zur Kryptogamenflora der Schweiz*. Vol. 4 (1). K.J. Wyss, Bern., pp. 1–254, 48 pls.
- Metzeltin, D. & Lange-Bertalot, H. (1998) Tropical diatoms of South America I. About 700 predominantly rarely known or new taxa representative of the neotropical flora. *Iconographia Diatomologica* 5: 1–695.
- Metzeltin, D. & Lange-Bertalot, H. (2007) Tropical Diatoms of South America II. Special remarks in the biogeographic disjunction.

*Iconographia Diatomologica* 18: 1–877.

- Müller, J., Müller, K., Neinhuis, C. & Quandt, D. (2010) PhyDE®—Phylogenetic data editor. Computer program. Available from: <http://www.phyde.de/> (accessed 11 March 2019)
- Nakov, T., Beaulieu, J.M. & Alverson, A.J. (2018) Accelerated diversification is related to life history and locomotion in a hyperdiverse lineage of microbial eukaryotes (Diatoms, Bacillariophyta). *New Phytologist* 219: 462–473.  
<https://doi.org/10.1111/nph.15137>
- Patrick, R.M. & Reimer, C.W. (1966) The diatoms of the United States exclusive of Alaska and Hawaii. Volume 1. Fragilariaceae, Eunotoniaceae, Achnantheaceae, Naviculaceae. *Monographs of the Academy of Natural Sciences of Philadelphia* 13: 688, 64 pls.  
<https://doi.org/10.2307/1351135>
- Pfitzer, E. (1871) Untersuchungen über Bau und Entwicklung der Bacillariaceen (Diatomaceen). In: Hanstein, J. (Ed.) *Botanische Abhandlungen aus dem Gebiet der Morphologie und Physiologie*. Bonn. p. 189.
- Reimer, C.W. (1959) The diatom genus *Neidium*. I. New species, new records and taxonomic revisions. *Proceeding of the Academy of Natural Sciences of Philadelphia* 111: 1–35, 4 pls.
- Ronquist, F. & Huelsenbeck, J.P. (2003) MrBayes 3: Bayesian phylogenetic inference under mixed models. *Bioinformatics* 19 (12): 1572–1574.  
<https://doi.org/10.1093/bioinformatics/btg180>
- Ross, R. (1947) Fresh water Diatomeae (Bacillariophyta). Botany of the Canadian Eastern Arctic II. N.V. Polunin (Ed.) *National Museum of Canada Bulletin* 97: 178–233, 3 pls.
- Schmidt, A. (1877) *Atlas der Diatomaceen-kunde*. Aschersleben: Verlag Von Ludwig Siever's Buchhandlung.  
<https://doi.org/10.5962/bhl.title.64396>
- Siver, P.A., Hamilton, P.B., Stachura-Suchoples, K. & Kocielek, J.P. (2003) Morphological observations of *Neidium* species with sagittate apices, including the description of *N. cape-codii* sp. nov. *Diatom Research* 18 (1): 131–148.  
<https://doi.org/10.1080/0269249X.2003.9705578>
- Skvortzow, B.W. (1936) Diatoms from Kizaki Lake, Honshu Island, Nippon. *Philippine Journal of Science* 61 (1): 9–73, 16 pls.
- Smith, W. (1853) *Synopsis of British Diatomaceae*. Vol. 1. John Van Voorst, London, 89 pp., pls. 1–31.
- Stosch, H.A. von. (1975) An amended terminology of the diatom girdle. *Nova Hedwigia* 53: 1–35.
- Theriot, E.C., Ashworth, M., Ruck, E., Nakov, T. & Jansen, R.K. (2010) A preliminary multigene phylogeny of the diatoms (Bacillariophyta): challenges for future research. *Plant Ecology and Evolution* 143 (3): 278–296.  
<https://doi.org/10.5091/plecevo.2010.418>